

# Possible Evidence of Asymmetry in SN 2007rt, a Type II<sub>n</sub> Supernova.

C. Trundle<sup>1</sup>, A. Pastorello<sup>1</sup>, S. Benetti,<sup>2</sup> R. Kotak<sup>1</sup>, S. Valenti<sup>1</sup>, I. Agnoletto<sup>2</sup>, F. Bufano<sup>2</sup>, M. Dolci<sup>3</sup>, N. Elias-Rosa<sup>4</sup>, T. Greiner<sup>5</sup>, D. Hunter<sup>1</sup>, F.P. Keenan<sup>1</sup>, V. Lorenzi<sup>6</sup>, K. Maguire<sup>1</sup>, S. Taubenberger<sup>7</sup>

<sup>1</sup> Astronomy Research Centre, Department of Physics & Astronomy, School of Mathematics & Physics, The Queen's University of Belfast, Belfast, BT7 1NN, Northern Ireland

<sup>2</sup> INAF Osservatorio Astronomico di Padova, Vicolo dell'Osservatorio 5, 35122 Padova, Italy

<sup>3</sup> Spitzer Science Center, California Institute of Technology, 1200 E. California Blvd., Pasadena, CA 91125, USA

<sup>4</sup> INAF Osservatorio Astronomico di Collurania, via M. Maggini, 64100 Teramo, Italy

<sup>5</sup> SLOOH Telescopes, 176 West Morris Road, Washington CT, 06793, USA

<sup>6</sup> Fundación Galileo Galilei-INAf, Telescopio Nazionale Galileo, 38700 Santa Cruz de la Palma, Tenerife, Spain

<sup>7</sup> Max-Planck-Institut für Astrophysik, Karl-Schwarzschild-Str. 1, 85741 Garching bei München, Germany

## ABSTRACT

An optical photometric and spectroscopic analysis of the slowly-evolving Type II<sub>n</sub> SN 2007rt is presented, covering a duration of 481 days after discovery. Its earliest spectrum, taken approximately 100 days after the explosion epoch, indicates the presence of a dense circumstellar medium, with which the supernova ejecta is interacting. This is supported by the slowly-evolving light curve. A notable feature in the spectrum of SN 2007rt is the presence of a broad He I 5875 line, not usually detected in Type II<sub>n</sub> supernovae. This may imply that the progenitor star has a high He/H ratio, having shed a significant portion of its hydrogen shell via mass-loss. An intermediate resolution spectrum reveals a narrow H<sub>α</sub> P-Cygni profile, the absorption component of which has a width of 128 km s<sup>-1</sup>. This slow velocity suggests that the progenitor of SN 2007rt recently underwent mass-loss with wind speeds comparable to the lower limits of those detected in luminous blue variables. Asymmetries in the line profiles of H and He at early phases bears some resemblance to double-peaked features observed in a number of Ib/c spectra. These asymmetries may be indicative of an asymmetric or bipolar outflow or alternatively dust formation in the fast expanding ejecta. In addition, the late time spectrum, at over 240 days post-explosion, shows clear evidence for the presence of newly formed dust.

**Key words.** supernovae: general – supernovae: individual (SN 2007rt)– circumstellar matter – stars: evolution, winds, outflow

## 1. Introduction

Stars with masses greater than 7-8 M<sub>⊙</sub> are thought to end their lives as core-collapse supernovae (CCSNe). During their lifetimes massive stars undergo significant mass-loss, particularly when massive enough to pass through a luminous blue variable (LBV) or Wolf-Rayet (WR) phase. Not surprisingly, this mass-loss leaves behind circumstellar material (CSM) surrounding the star.

Evidence for the presence of surrounding CSM has been detected in a number of hydrogen rich SNe. The spectra of these objects do not show the broad P-Cygni profiles of the prototypical Type II supernovae. Instead, they are distinguished by their narrow H<sub>α</sub> emission (< 1000 km s<sup>-1</sup>) on top of a broader emission profile. This narrow feature is a signature for the presence of circumstellar matter previously shed by the progenitor star. Such objects led Schlegel (1990) to identify a sub-class of objects amongst the hydrogen rich core-collapse supernovae, namely Type II<sub>n</sub>.

It is now generally believed that if a star undergoes significant mass-loss in its lifetime and subsequently evolves into a supernova, the fast moving ejecta from the explosion interacts with the discarded wind-material. This interaction is believed to cause a fast shock wave in the CSM and a reverse shock in the ejecta, with the shocked regions emitting high energy ra-

diation (Chevalier & Fransson 1994; Chugai & Danziger 1994). The intensity of this interaction and its effect on the supernova spectrum and light-curve is dependent on the density, composition and geometrical configuration of the CSM, and can provide an excellent trace of the mass-loss in the pre-explosion lifetime of the progenitor star. Type II<sub>n</sub> SNe constitute a very heterogeneous group of objects showing a wide variation in the strengths of their emission lines and behaviour of their light curves. Whilst the prototype II<sub>n</sub>, SN 1988Z (Stathakis & Sadler 1991; Turatto et al. 1993; Aretxaga et al. 1999) is less luminous than Type Ia SNe, some of the most luminous SNe belong to this class (viz. 2006gy, 2006tf; see Ofek et al. 2007; Smith et al. 2007, 2008a; Agnoletto et al. 2009).

In addition to the characteristic narrow H features, type II<sub>n</sub> spectra generally have strong blue continua, to which a single blackbody can not provide an adequate fit whilst simultaneously fitting the red part of the spectrum. Smith et al. (2009a) suggested that at late times the blue continuum present in the type II<sub>n</sub> SN 2005ip was a result of the presence of a forest of high ionisation forbidden emission lines and they refer to this as a pseudo-continuum. This verified earlier speculation by Stathakis & Sadler and Turatto et al. that the source of the blue spectral region in SN 1988Z was a strong interaction with the surrounding circumstellar material.

The presence of CSM provides a unique insight into the mass-loss history of the progenitor prior to core-collapse.

However, there remains an element of ambiguity over the progenitors of type II<sub>n</sub> supernovae. Recent work has indicated that some of these objects may be connected to luminous blue variables (LBVs) or at least have undergone LBV-like behaviour shortly before core-collapse (see Kotak & Vink 2006; Gal-Yam et al. 2007; Gal-Yam & Leonard 2008; Smith et al. 2007; Trundle et al. 2008; Smith et al. 2008a; Agnoletto et al. 2009). Another group, the hybrid Type Ia/II<sub>n</sub>, are thought to be a Type Ia disguised as a Type II<sub>n</sub>, due to the strong narrow  $H_{\alpha}$  emission in their spectra and the possible presence of the S II and Si II features typical of Type Ia (viz. SN 2002ic; see Hamuy et al. 2003; Aldering et al. 2006; Kotak et al. 2004). However, this is largely under debate within the community (Benetti et al. 2006; Trundle et al. 2008). There are also a number of so-called ‘transitional’ objects, where the presence of varying degrees of narrow hydrogen and helium lines in their spectra place them in a classification scheme between Type II<sub>n</sub> and Type Ib/c objects (such as SN 2005la and the type Ibn, SN 2006jc Pastorello et al. 2007; Foley et al. 2007; Pastorello et al. 2008a,b; Smith et al. 2008b). The ambiguities surrounding Type II<sub>n</sub> progenitors leads us to tread carefully whilst discussing this group of supernovae, and justifies an in-depth analysis of those in the class which are dissimilar to the groups prototype, SN 1988Z (Stathakis & Sadler 1991; Turatto et al. 1993; Aretxaga et al. 1999).

In this paper we will discuss the photometric and spectroscopic evolution of SN 2007rt, for more than 400 days post-discovery. SN 2007rt was discovered by Li (2007) in UGC 6109, from unfiltered KAIT images on the 24<sup>th</sup> November 2007. Blondin (2007), as part of the CfA Supernova Survey, classified SN 2007rt as a type II<sub>n</sub> supernova, 2-3 months past maximum, and claim the two best comparison spectra for this object are of the type II<sub>n</sub>’s SN 1998S and 1996L. However from followup spectra we identified a broad helium feature, which is not detected in SN 1998S or many other type II<sub>n</sub> SNe, and hence warrants further investigation.

## 2. Observations

Photometric and spectroscopic data of SN 2007rt were collected from November 2007 to March 2009. The details of these observations are logged in Table 1 and are outlined below.

### 2.1. Photometry

Our collaboration obtained optical photometry of SN 2007rt with the Telescopio Nazionale Galileo (TNG) and Nordic Optical Telescope (NOT) in La Palma (Canary Islands, Spain), the 1.82m Copernico telescope of the Asiago Observatory (Italy), the 1.52m telescope of the Loiano Observatory (Italy), and the 2.2m Calar Alto telescope (Spain). In addition four data points provided by amateur astronomers were used. In total this gives a coverage from 4 to 481 days after discovery (see Fig. 1). The images were trimmed, de-biased and flatfielded. Since template images of the host galaxy were not available, the SN magnitudes were measured using a point spread function (PSF) fitting technique in the Image Reduction and Analysis Facility (IRAF)<sup>1</sup>. Zero-points were defined making use of standard Landolt fields observed on the same night as the SN. The

<sup>1</sup> IRAF is distributed by the National Optical Astronomy Observatories, which are operated by the Association of Universities for Research in Astronomy, Inc., under cooperative agreement with the National Science Foundation.

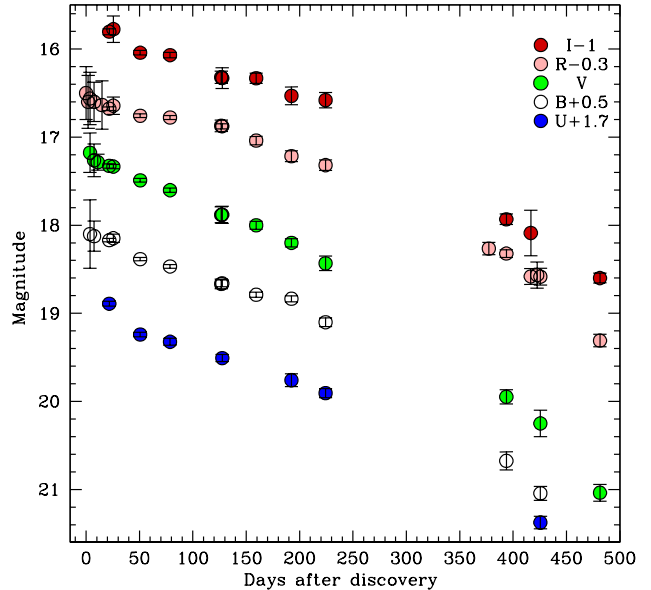


Fig. 1: UBVR light curves of SN 2007rt up to 481 days after discovery. From top to bottom the points are I, R, V, B, and U with offsets of -1, -0.3, 0, +0.5 and +1.7 mag. respectively. The discovery magnitudes reported by Li (2007) are also included here.

magnitudes of SN 2007rt were then calibrated relative to the average magnitudes of a sequence of stars in the SN field obtained during three photometric nights (highlighted by (ph) in column 7 of Table 1). Unfiltered magnitudes obtained from amateur images were rescaled to the V or R band magnitudes depending on the wavelength position of the maximum of the quantum-efficiency curve of the detectors used (see also the discussion in Pastorello et al. 2008c). These unfiltered magnitudes are denoted by C in Table 1. The calibrated SN magnitudes are presented in Table 2 and Fig. 1.

### 2.2. Spectroscopic Data

An intermediate resolution ( $\sim 30 \text{ km s}^{-1}$ ) optical spectrum of SN 2007rt was obtained using the William Herschel telescope (WHT) on La Palma, as well as low resolution ( $\sim 200 \text{ km s}^{-1}$ ) spectra from the telescopes listed above for photometry. These provided spectral coverage over a 426 day period from discovery on 24<sup>th</sup> November 2007. Details of the epoch, wavelength coverage and resolution of these spectra are presented in Table 1. The spectra were reduced using standard spectral reduction procedures in IRAF. They were wavelength and flux calibrated using arc lamps and spectrophotometric standards observed on the same night. The wavelength calibrations were verified using the narrow sky lines. Absolute flux calibrations were then made with photometry taken on the same night. Prior to flux calibration, it was necessary to apply a second order correction to the ALFOSC/NOT spectra, due to contamination in the red part of the spectra from blue light of the second order. This was accomplished using the procedure outlined by Stanishev (2007).

The spectroscopic data have been corrected for the redshift of the host galaxy, UGC 06109 ( $z=0.022365 \pm 0.00080$ ) as published in the updated Zwicky catalog (Falco et al. 1999). The blue continuum plus absence of Na I D lines in the spectra of

Table 1: Log of photometric and spectroscopic observations of SN 2007rt.

DATE	Phase (days)*	Telescope/Instr	Spectroscopy			Photometry
			Grism	Wav. Range (Å)	Res.(Å)	
28-11-2007	85	(1)				BVRC
02-12-2007	89	(1)				BVRC
05-12-2007	92	(2)				VC
09-12-2007	96	(3)				C
15-12-2007	102	TNG/Dolores	LRB+LRR	3200-9600	17	UBVRI (ph)
19-12-2007	106	Loiano1.52/BFOSC	gm4+gm5	3500-9600	14	BVR (ph)
13-01-2008	131	NOT/ALFOSC	gm4	3300-8900	13.5	UBVRI
04-02-2008	153	WHT/ISIS	R1200R	6000-6850	0.7	
11-02-2008	160	TNG/Dolores	LRB+LRR	3200-9600	9	UBVRI
29-03-2008	207	Ekar1.82/AFOSC				BVRI
30-03-2008	208	NOT/ALFOSC	gm4	3300-8900	16.5	UBVRI
29-04-2008	238	Loiano1.52/BFOSC	gm4+gm5	3600-8700	13	
01-05-2008	240	CAHA/CAFOS	b200	3300-8900	13	BVRI
03-06-2008	273	CAHA/CAFOS	b200	3300-8900	13	UBVRI
07-07-2008	307	CAHA/CAFOS				UBVRI (ph)
05-12-2008	458	NOT/ALFOSC				R
22-12-2008	475	TNG/Dolores	LRR	4950-9600	13	BVRI
13-01-2009	497	TNG/Dolores	LRB	3400-7750	15	RI
20-01-2009	504	TNG/Dolores				R
22-01-2009	506	TNG/Dolores	LRB	3500-7900	12	
23-01-2009	507	TNG/Dolores	LRB+LRR	3400-9500	12	UBVR
19-03-2009	562	CAHA/CAFOS				BVRI

(1)0.35m f/11 Schmidt-Cassegrain telescope+Kodak KAF-3200ME CCD, SLOOH, Teide Observatory, Canary Islands, Spain; (2)0.25m f/3.8 Takahashi Epsilon telescope E250+SBIG ST-8XE CCD - Remote Astronomical Society Observatory, New Mexico, USA; (3)0.37m f14 Cassegrain Iowa Robotic Telescope+ FLI PL-09000 CCD, Winer Observatory, Arizona & University of Iowa, USA

\* Phase refers to the number of days post-explosion, assuming a discovery date of 81 days post-explosion.

Table 2: Optical photometry of SN 2007rt.

DATE	Phase(days)	U	U <sub>err</sub>	B	B <sub>err</sub>	V	V <sub>err</sub>	R	R <sub>err</sub>	I	I <sub>err</sub>
28-11-2007	85			17.600	0.388	17.177	0.224	16.862	0.297		
02-12-2007	89			17.624	0.172	17.263	0.186	16.900	0.222		
05-12-2007	92					17.285	0.090				
09-12-2007	96							16.935	0.273		
15-12-2007	102	17.191	0.027	17.670	0.019	17.327	0.025	16.977	0.021	16.803	0.033
19-12-2007	106			17.648	0.046	17.334	0.023	16.943	0.098	16.744	0.150
13-01-2008	131	17.541	0.026	17.885	0.018	17.490	0.021	17.057	0.021	17.042	0.026
11-02-2008	160	17.623	0.039	17.968	0.020	17.602	0.023	17.077	0.022	17.069	0.030
29-03-2008	207			18.166	0.054	17.882	0.090	17.171	0.066	17.321	0.070
30-03-2008	208	17.808	0.041	18.160	0.039	17.881	0.097	17.176	0.028	17.329	0.118
01-05-2008	240			18.289	0.028	18.001	0.045	17.339	0.047	17.331	0.059
03-06-2008	273	18.059	0.073	18.335	0.034	18.200	0.047	17.516	0.061	17.531	0.101
07-07-2008	307	18.206	0.051	18.601	0.049	18.433	0.082	17.618	0.059	17.580	0.087
05-12-2008	458							18.565	0.070		
22-12-2008	475			20.175	0.102	19.948	0.082	18.622	0.043	18.932	0.060
13-01-2009	497							18.881	0.090	19.088	0.258
20-01-2009	506							18.866	0.148		
23-01-2009	507	19.675	0.071	20.543	0.079	20.250	0.149	18.884	0.096		
19-03-2009	562			21.179	0.103	21.012	0.095	19.610	0.071	19.600	0.055

The phase is given relative to the explosion date, believed to be 81 days prior to the discovery date on 24<sup>th</sup> November 2007.

SN 2007rt suggest that there is a negligible effect due to extinction on the observed spectral energy distribution. Thus we have only corrected the spectra by the small Galactic extinction contribution as suggested by Schlegel et al. (1998). Along the line of sight of SN 2007rt the Galactic extinction is  $E(B-V) = 0.02$ .

### 3. Light Curve evolution

Fig. 1 shows the UBVRI light curves of SN 2007rt. Over the first 130 days after discovery, the light curve of SN 2007rt evolves slowly (at a rate of  $0.003 \text{ mag d}^{-1}$ ) and it is clear the supernova has not be caught at maximum (see Sect. 4). Following this there is a gradual decline in the light curve, which steepens at late phases ( $0.01 \text{ mag d}^{-1}$  from 458-562 days post-explosion). It was reported by Li (2007) that on a KAIT image taken almost

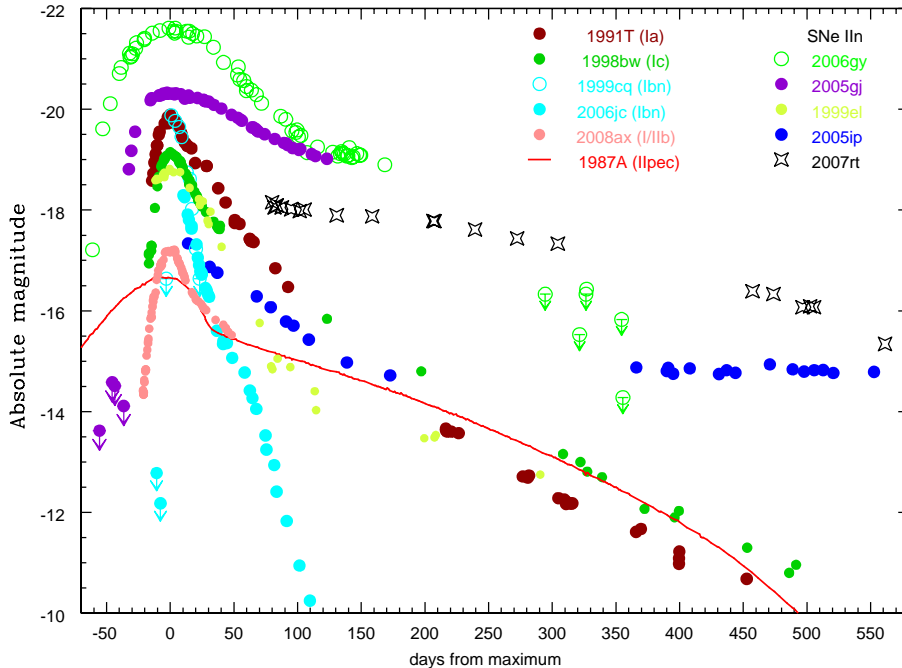


Fig. 2: Absolute R band magnitudes of SN 2007rt compared to a range of SN types. Reference of the SNe magnitudes are: SN 1987A - Whitelock et al. (1989, and references therein), SN 1991T - Schmidt et al. (1994); Cappellaro et al. (1997); Sparks et al. (1999), SN 1998bw - Galama et al. (1998); McKenzie & Schaefer (1999); Sollerman et al. (2000); Patat et al. (2001), SN 1999cq - Matheson et al. (2000), SN 2006jc - Pastorello et al. (2007); Foley et al. (2007), SN 2008ax - Pastorello et al. (2008c), and the Type IIn’s SN 1999el - Di Carlo et al. (2002), SN 2005gj - Aldering et al. (2006); Prieto et al. (2007), SN 2005ip - Smith et al. (2009a), SN 2006gy - Smith et al. (2007); Ofek et al. (2007); Agnoletto et al. (2009); Kawabata et al. (2009).

seven months prior to discovery, on 8<sup>th</sup> May 2007, nothing was detected at the position of the supernova. Since this supernova has been discovered quite late on in its evolution, as suggested by the non-detection of a maximum in the light curve, it is difficult to determine the explosion epoch. However we obtained an estimate of the explosion date of SN 2007rt indirectly using the spectra and light-curve of an interacting type IIn SN, SN 2005ip.

### 3.1. Age of SN 2007rt

The light-curve of SN 2005ip declined rapidly after discovery, suggesting SN 2005ip was discovered close to maximum (Smith et al. 2009a). Many core collapse SNe, for which the rise time to peak was observed, have rise times of 3 weeks or less. Few SNe Type IIn have been detected during this rise phase, and those that have, give rise times of 20-50 days (see SN 2006gy and SN 2005gj in Fig. 2). The fact that type IIn are rarely detected before maximum, suggests that the rise time is quite fast. Based on this, it is reasonable to assume that SN 2005ip was detected within a couple of weeks from explosion. Hence we adopt an explosion date for SN 2005ip of JD=2453673, which is 7 days prior to its detection (Fig. 2). This is consistent with the findings of Smith et al., however we cannot ignore that there is a large degree of uncertainty in this. The assumption of a short rise time of SN2005ip is also supported by the rapid change in the spectra after discovery. The first spectrum shows an almost featureless and very blue spectrum (Smith et al. 2009a) and over the following days the broad features and continuum evolve rapidly (from unpublished spectra, Trundle et al. in prep).

At 95 days after its discovery, the spectrum of SN 2005ip best fits the broad features and slope of our first SN 2007rt spectrum (see Sect. 5.1). Assuming the similarity of the spectra of SN 2005ip and SN 2007rt indicates that these supernovae are of similar age, the age estimate of the first spectral epoch of SN 2007rt can be refined to approximately  $102 \pm 40$  days after explosion, and thus the explosion date is set to JD=2454349  $\pm$  40. Before adopting this age, for the following discussions, we will attempt to qualify our assumption that these two objects are close to or of a similar age at these epochs. The spectra of SN 2007rt at discovery and SN 2005ip at 95 days are heavily dominated by the CSM interaction. So although there is evidence for spectral similarity the properties of the CSM may mask the true epoch. However a very young age can be ruled out for SN 2007rt. Firstly, the first spectrum was obtained 21 days post-discovery and hence SN 2007rt must be at least 21 days old. Secondly, in an early epoch (<40 days) Type IIn, a strong blue continuum would be expected which evolves rapidly along with the broad features (viz. SN 2005ip, SN 2005gj; Smith et al. (2009a); Aldering et al. (2006)). However the blue continuum and broad features in SN 2007rt, do not evolve rapidly over a 60 day period between our first and fifth spectrum (see further discussion on continuum Sect. 4). Similarly a large amount of CSM, prolonging the interaction duration of SN 2007rt could lead to an underestimate of its age. In spite of this, uncertainties of a few weeks in our estimates will not substantially alter our findings. From this point forward we adopt the explosion date of JD=2454349  $\pm$  40, implying the observations of SN 2007rt were taken between 85 to 562 days post-explosion.<sup>2</sup>

<sup>2</sup> All dates in the rest of this article refer to the adopted explosion epoch, unless otherwise stated.

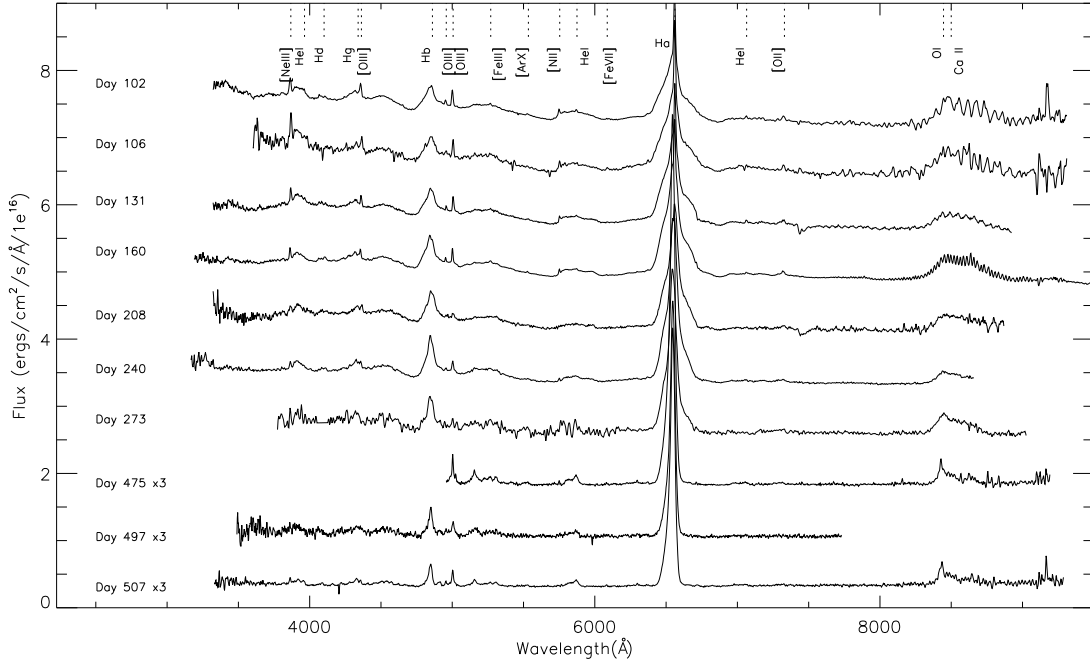


Fig. 3: Dereddened optical spectra of SN 2007rt from 102 to 507 days after its adopted explosion date. Flux for each spectrum is arbitrarily offset by 0.75 for clarity, and the spectra from days 475, 497, & 507 are scaled by a factor of 3 in flux.

The light curve of SN 2007rt is compared to those of a range of SNe types in Fig. 2. At approximately 100 days past maximum, SN 2007rt is more luminous than the fast-declining type II in SN 1999el, but fainter than some of the most luminous type II in objects, SN 2006gy and SN 2005gj. Despite the similarity in the spectra of SN 2007rt and SN 2005ip at early times, there is a significant difference in the absolute luminosity of their light curves. This may be caused by differing densities and distributions of circumstellar matter surrounding the two SNe. The early time light-curve evolution of SN 2007rt is very slow, declining by  $0.003 \text{ mag d}^{-1}$ . This is considerably slower than SN 2005ip which has a decline rate for a similar period of  $0.015 \text{ mag d}^{-1}$  (Smith et al. 2009a).

#### 4. Spectral evolution

The spectra of SN 2007rt, displayed in Fig. 3, have been corrected for a Galactic reddening of  $E(B-V) = 0.02 \text{ mag}$  as discussed in Sect. 2.2. There is a blue excess present in the spectra in the early epochs, which flattens after more than 300 days post-explosion. We fit a blackbody to the spectrum of SN 2007rt, and obtain a temperature of  $\sim 7500 \text{ K}$  for the first epoch. This fit in itself was poor and as the SN evolved it became increasingly difficult to simultaneously reconcile the flat red spectral region and the blue excess with a single blackbody. Smith et al. (2009a) showed that, in the case of SN 2005ip, spectra taken some 200 days after maximum revealed a blue pseudo-continuum composed of a forest of narrow emission lines, rather than a real thermal continuum with a blackbody like behaviour. This indicated that for SN 2005ip the blue pseudo-continuum at late times arose from the interaction with circumstellar material, and was not a real thermal continuum. This had previously been speculated by Stathakis & Sadler (1991) and Turatto et al. (1993) for the case of SN 1988Z. The low velocity of the CSM in SN 2005ip al-

lowed the detection of the separate components of the emission line spectrum in the blue which formed the pseudo-continuum at late-stages. It therefore may be possible that the temperature derived by fitting a blackbody to the spectrum of SN 2007rt is not meaningful. This will be discussed further in Sect. 5.1.<sup>3</sup>

Prominent features in the spectra of SN 2007rt are the narrow and broad  $H_{\alpha}$  features, the intermediate velocity  $H_{\beta}$  line and broad Ca II infrared triplet. There are also a number of narrow emission features associated with He and heavier metals in the spectra. However, possibly the most peculiar spectral feature is the broad, relatively flat topped He I 5875 Å emission line. In Fig. 3 these main features are identified. At all phases the H and He lines are asymmetric. At late times the  $H_{\alpha}$  and He I 5875 Å lines have a pronounced blueshift, and a significant lack of redshifted emission in the broad component. There is also a hint of a narrow component of He I 5875 and 7065 Å in the early epochs (see Fig. 4), suggesting there is a certain amount of helium in the CSM. The narrow He I 5875 Å line diminishes from the first spectra (102 days post-explosion), and disappears by day 208. In the later epochs, from day 475, an intermediate velocity component appears. This suggests that there is interaction between the ejecta and the He in the CSM. In addition, a strong permitted O I 8446 Å line develops from day 273, which has velocities comparable to the intermediate H component.

To determine the properties of the spectral features we have fit Gaussians to their profiles. Each Gaussian was parameterized by three quantities, the central wavelength, full-width-half-maximum (FWHM) and peak height. These parameters were freely fit by the fitting routine. In a small number of cases, the

<sup>3</sup> From this point forward the term continuum refers to the overall shape of the spectrum, while ‘thermal continuum’ and ‘pseudo-continuum’ are used to distinguish between a thermal blackbody like continuum and an unresolved forest of emission lines.

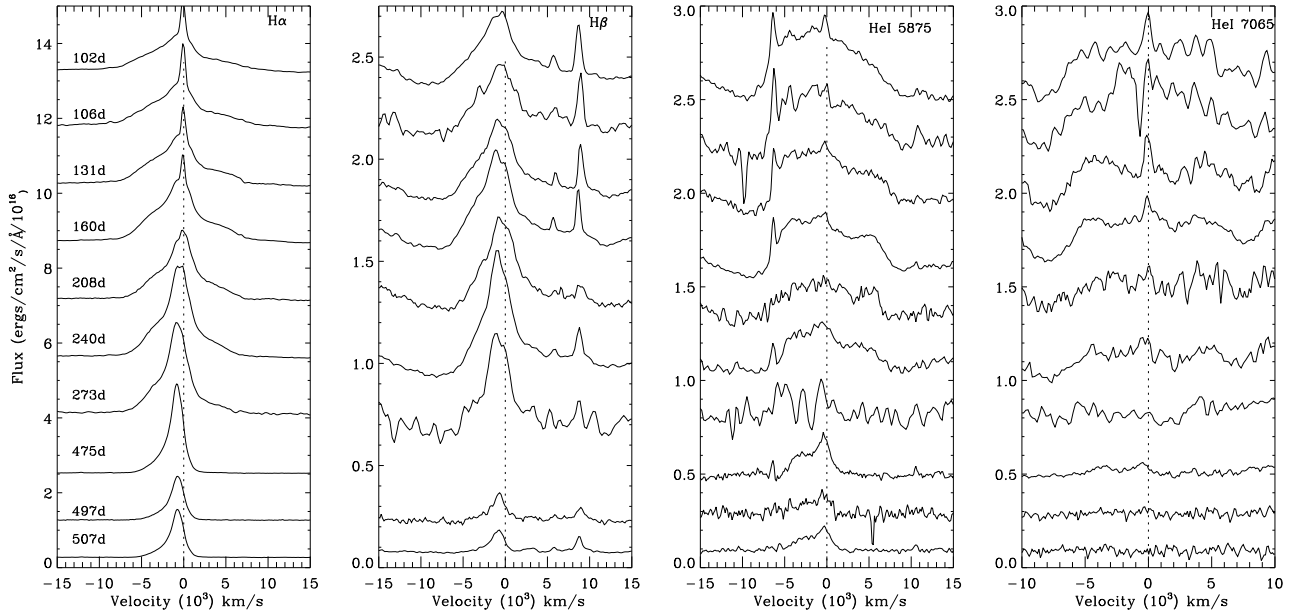


Fig. 4: Observed  $H_\alpha$ ,  $H_\beta$ , He I 5875 Å and He I 7065 Å profiles in SN 2007rt from 102 to 507 days since the explosion date. The flux of each spectrum is arbitrarily offset for clarity. Note the blue-shift in the later epochs of  $H_\alpha$  and the asymmetry in its red wing. In the last two panels, the flux has been magnified by a factor of 4 for an easier view of the weak narrow helium features. Note under magnification there appears to be a weak broad helium component at 7065 Å.

central wavelengths of the narrow lines were fixed, as the low intensity of the line relative to the continuum prohibited the detection of its peak. The resulting wavelengths, velocities and intensities of the lines are presented in Tables 3 - 5. All FWHM given in the aforementioned tables and the discussions below are corrected for the instrumental resolution. In interacting supernovae the flux calibration is subject to large uncertainties due to the presence of strong emission lines. Errors on the measured intensities of the lines are therefore on the order of 20%, whereas the FWHM uncertainties are 10%. The narrow lines which were detected and fitted in the spectrum had FWHM velocities that were not fully resolved by the low resolution spectra (these are discussed further in Sect. 4.4). As a guide to the properties of these lines, their parameters as determined from the TNG spectrum taken on the 11<sup>th</sup> February are presented in Table 5. In addition a number of the lines were resolved in the intermediate resolution WHT spectrum taken on the 4<sup>th</sup> February, and these are also presented in the aforementioned table.

In the case of  $H_\alpha$  and He I 5875 Å, multiple Gaussian fits were employed (see Sect. 4.2) due to the asymmetry of the observed profiles. As discussed in more detail below,  $H_\alpha$  was first fit with a broad, intermediate and narrow Gaussian whilst the He I 5875 Å line was fit with a broad and narrow component for the early epochs, and a broad and intermediate component for the latest epochs. The parameters of the broad and intermediate components from these fits are shown in Table 3. However these initial fits were poor, and hence we refit the profiles with up to four Gaussians; an intermediate component, two broad components, and where appropriate a narrow component. The parameters of the broad and intermediate components of the latter fits are presented in Table 4.

#### 4.1. Narrow $H_\alpha$ P-Cygni profile

Fig. 4 shows the time-series of the  $H_\alpha$  line. From day 102 to day 208 there is a narrow emission component present which decreases in strength over time. The luminosity of this narrow component decreases by more than a factor of 2 between our first epoch of data and that taken 58 days later. It has disappeared completely 138 days after our first spectrum. This feature is not fully resolved by the low resolution spectra which makes up most of our dataset. However, we can place an upper limit on the FWHM velocity of  $\leq 200 \text{ km s}^{-1}$  (see Table 5).

To resolve this narrow  $H_\alpha$  feature we obtained intermediate resolution spectra of SN 2007rt on the 4<sup>th</sup> February 2008 with ISIS on the WHT. This revealed a previously unresolved P-Cygni profile (see Fig. 5). The FWHM of the emission and absorption feature are 84 and 54  $\text{km s}^{-1}$ , respectively (Table 5). The blue wing of the absorption profile extends out to 128  $\text{km s}^{-1}$ . If we assume that the narrow feature is representative of unshocked CSM, this edge velocity of 128  $\text{km s}^{-1}$  corresponds to the terminal velocity of the wind of the progenitor star (see Sect. 5.3 for more discussion on the progenitor).

#### 4.2. $H_\alpha$ and He I evolution

From the  $H_\alpha$  profiles in the first panel of Fig. 4, we can see that the line is highly asymmetric and consists of multiple components. Typically, the  $H_\alpha$  profile of Type II<sub>n</sub> supernovae can be decomposed into three parts: broad, intermediate and narrow. These are normally attributed to shocked (intermediate) and unshocked (narrow) circumstellar matter and emission from the underlying supernova ejecta (broad). In SN 2007rt, the red wing of the broad feature appears to be less extended than the blue wing, and both the broad and intermediate features show some asymmetry. The extent of the blue and red wings decrease rapidly with

Table 3: Initial parameters for the intermediate and broad Gaussian fits to spectral lines in SN 2007rt.

Line	Day	$\lambda$ Å	FWHM km s <sup>-1</sup>	Intensity 10 <sup>-15</sup> erg.s <sup>-1</sup> cm <sup>2</sup>
He I 3926 broad	102	3919.12	7340	13.43
	106	3919.36	6482	16.95
	131	3924.15	6463	11.85
	160	3918.89	6004	8.63
	208	3925.70	4850	6.97
	240	3921.51	4948	7.76
	273	3930.00	4155	6.53
H $\gamma$ 4340 Inter.	102	4318.15	5808	9.39
	106	4321.20	5114	6.31
	131	4316.22	4851	6.99
	160	4317.16	5683	7.37
	208	4344.80	4649	6.74
	240	4330.00	4743	6.76
	497	4337.32	3992	1.16
H $\beta$ 4861 Inter.	102	4847.43	3850	15.31
	106	4852.75	4151	16.80
	131	4851.27	4046	19.64
	160	4847.14	4099	24.52
	208	4856.45	3638	20.63
	240	4852.49	3258	24.78
	273	4852.13	2678	16.04
	497	4851.03	1673	2.98
	507	4849.14	1614	2.35
He I 5875 broad	102	5860.11	10279	24.11
	106	5872.61	9640	20.77
	131	5870.01	9729	19.05
	160	5869.47	10146	17.89
	208	5872.93	9834	11.56
	240	5867.50	8080	11.07
	475	5837.26	4466	1.74
	497	5848.50	4538	1.77
	507	5835.03	4057	1.58
He I 5875 Inter.*	475	5872.62	1072	0.63
	507	5872.61	1318	0.52
H $\alpha$ 6563 broad	102	6543.71	10136	121.68
	106	6546.19	10113	145.75
	131	6545.41	8793	145.94
	153	6543.88	8244	139.41
	160	6550.00	8489	179.92
	208	6553.00	7285	149.68
	240	6548.34	6835	171.70
	273	6541.33	6047	129.30
	475	6529.07	3645	42.87
	497	6530.32	3593	26.61
	507	6530.72	3495	28.93
H $\alpha$ 6563 Inter.	102	6548.29	2905	24.11
	106	6552.01	2687	27.02
	131	6555.53	2179	24.30
	153	6555.35	2195	29.38
	160	6554.89	2212	33.85
	208	6562.25	1734	33.40
	240	6557.58	1824	53.87
	273	6553.28	1812	53.08
	475	6549.65	1353	40.20
	497	6551.11	1357	26.40
	507	6550.96	1335	27.72
O I 8446 inter.	273	8441.22	2980	12.59
	497	8433.39	1399	3.15
	507	8434.35	1244	2.45
Ca II broad	102	8550.00	12982	118.48
	106	8540.47	11541	101.92
	131	8553.22	11651	72.96
	160	8552.43	12486	117.55
	273	8544.40	8750	44.89
	475	8535.883	8570	7.32

\* An intermediate He I 5875 Å line was detected at 475 & 507 days. Prior to that only weak narrow and broad components were present.

time, showing a reduction in the FWHM of the broad component, and hence a change in the ejecta. There is also a notable blueshift in the 240 day spectrum, which becomes more pronounced by day 273, and which is accompanied by an increased asymmetry or decrease in the emission in the red wing. In the latest epochs, between 475 and 507 days, the blueshift is still present and there is a remarkable lack of redshifted emission. This change in the line profiles is accompanied by a simultaneous decline in the light curve of SN 2007rt (see Fig. 2). Asymmetry in the line profile and a blue-shifted peak are often related to dust formation. Since this affects the broad component of the line it could indicate the presence of newly formed dust in the SN ejecta (viz. SN 1987A; see Danziger et al. 1989; Lucy et al. 1989).

In the first instance the complex profile of H $\alpha$  in SN 2007rt was fit with three Gaussian profiles allowing all parameters to be freely fit. In the early epochs, the He I 5875 Å line did not require an intermediate component and hence was fit only with components representing the broad and narrow features. An additional narrow component was added to account for the contribution to the profile from [N II] 5755 Å. In the case of He I 5875 Å the central wavelength of the narrow component was fixed. The narrow line is no longer present in either the H or He lines after 208 days, and hence the profiles at these epochs were fit with only two Gaussians (see Fig. A.2<sup>4</sup>). From day 475, two Gaussians were fit to the He I 5875 Å line representing the broad and intermediate components. The top panel of Fig. 6 shows a typical fit to H $\alpha$  for one epoch. The parameters determined from this process for the intermediate and broad components are reported in Table 3, those of the narrow components are presented separately. Uncertainties in the central wavelengths, FWHM, and intensities of the fits are  $\pm 5$ -7 Å, 10%, and 20%, respectively. The intermediate component has a FWHM velocity range of  $\sim 2900$  - 1800 km s<sup>-1</sup> over the first 192 days from discovery. There is a gradual reduction in the FWHM of the broad components of the two lines over the observed period. In the first spectrum the broad component has a FWHM velocity of  $\sim 10,000$  km s<sup>-1</sup>, decreasing to 6000 km s<sup>-1</sup> 171 days later (see upper panel of Fig. 7). The fact that there is nearly a 40% reduction in the width of the line clearly shows that this broad component is related to the ejecta. Nevertheless, the high velocity of 10,000 km s<sup>-1</sup> detected over three months after explosion is inconsistent with non-interacting CCSNe and requires an extremely energetic explosion. We note here that the high expansion velocities are only inconsistent if the age of SN 2007rt is greater than a month or two. However as discussed in Sect. 3.1 we cannot provide an accurate age estimate of the SN, the implications of these assumptions will be discussed further in Sect. 5.4.

Careful inspection of Fig. 6 reveals that the combination of the three Gaussian profiles does not provide a suitable fit to the red wing of the H $\alpha$  profile. In addition, the peculiarly flat-topped He I mentioned in Sect.4 is not consistent with a single broad component. An enhanced fit to both lines was found by fitting up to four Gaussian profiles: an intermediate component, broader blue and red-shifted components, and where appropriate, a narrow component (see Fig. 6). The significance of these fits will be discussed in more detail in Sect. 5, but briefly the two components at rest represent the shocked and unshocked circumstellar material. The other two components represent blobs of higher velocity material moving away from the supernova, one in the direction of the observer and one opposite to this. To produce

<sup>4</sup> Fig. A.2 is only available online

Table 4: Parameters of the multiple Gaussian fits to the  $H_\alpha$  and He I 5875 Å lines, using four gaussian profiles (2 broad, 1 intermediate & 1 narrow)

Line	Day	$\lambda$ Å	FWHM km s <sup>-1</sup>	Intensity 10 <sup>-15</sup> erg.s <sup>-1</sup> cm <sup>2</sup>
He I 5875 Broad Blue	102	5805.66	5838	11.31
	106	5797.95	5782	8.95
	131	5809.73	5081	8.86
	160	5812.44	4720	8.23
	208	5811.79	4007	4.66
	240	5816.00	3939	4.58
	475	5822.00	2285	1.77
	497	5819.72	2134	0.83
507	5821.83	2123	0.82	
He I 5875 Intermediate	102	5869.19	2708	2.65
	106	5864.20	2771	2.71
	131	5875.50	2653	3.12
	160	5876.78	2726	2.14
	208	5875.50	2515	2.96
	240	5875.97	2509	2.95
	475	5870.52	1688	1.00
	497	5869.66	1703	1.00
507	5871.27	1691	0.99	
He I 5875 Broad red	102	5943.84	6712	10.65
	106	5936.13	6966	9.66
	131	5947.91	5556	6.61
	160	5950.42	5670	7.88
	208	5949.97	3930	3.90
240	5953.43	3593	2.85	
$H_\alpha$ 6563 Broad blue	102	6500.00	5838	69.62
	106	6500.00	5782	78.98
	131	6500.00	5081	78.22
	160	6500.00	4720	85.95
	208	6500.00	4007	56.47
	240	6500.00	3939	67.47
	273	6500.00	3808	53.66
	475	6500.00	2285	16.84
	497	6500.00	2134	9.72
507	6500.00	2123	10.59	
$H_\alpha$ 6563 Intermediate	102	6563.53	2708	32.01
	106	6566.25	2771	39.45
	131	6565.77	2653	51.14
	160	6564.34	2726	71.04
	207	6563.71	2515	85.36
	240	6559.97	2509	119.14
	273	6555.55	2436	108.15
	475	6548.88	1688	64.16
	497	6549.72	1703	41.66
507	6549.44	1691	45.07	
$H_\alpha$ 6563 Broad red	102	6638.18	6712	38.64
	106	6638.18	6966	47.82
	131	6638.18	5556	41.83
	160	6638.18	5670	55.25
	207	6638.18	3930	35.68
	240	6638.18	3593	35.80
273	6638.18	3697	22.10	

Only parameters of intermediate and broad components are presented here. Narrow components are in Table 5.

these fits, the  $H_\alpha$  line was fit with multiple components, fixing the central wavelengths of the blue and red -shifted broad components in an iterative manner, whilst the other parameters were set free. For the helium line, the FWHM and separation of the broad and intermediate components determined for the  $H_\alpha$  line, were used to fix their counterparts in the He I feature. The lower panels of Fig. 6 show the resultant fits to  $H_\alpha$  and He I 5875 Å. (Fits to the spectra for additional epochs can be seen

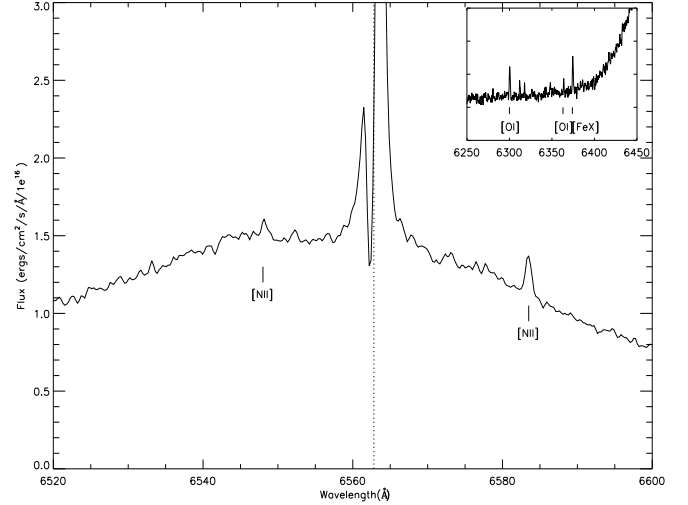


Fig. 5: Intermediate resolution WHT/ISIS spectra of SN 2007rt at 153 days post-explosion, centered on the  $H_\alpha$  region. Note the narrow P-Cygni profile not detected in the low resolution spectra presented in Fig. 4. A number of narrow metal line features were also detected in this wavelength range: [N II] 6548, 6583 Å, [O I] 6300, 6343 Å and [Fe X] 6374 Å (see inset).

in Fig. A.3, which is only available online). The parameters for the intermediate and broad components are presented in Table 4. In the first epoch the intermediate component in both profiles has a FWHM of  $\sim 2700$  km s<sup>-1</sup>, whilst the blue and red-shifted broader components are at  $\sim 5800$  and  $6700$  km s<sup>-1</sup>, respectively (see Table 4 and lower panel of Fig. 7). Over the first six months of the observational period of SN 2007rt, the broad component shows a 40% reduction in FWHM, whereas the intermediate component does not experience any noticeable change. It is therefore clear that the broader components are related to the ejecta, whilst the intermediate component is consistent with shocked material. In the last epochs taken a further 6 months later, only two components (a blue-shifted broad and intermediate component) were used to fit the data due to a lack of emission in the red wing of the lines.

### 4.3. $H_\beta$

A strong intermediate component of  $H_\beta$  is detected in SN 2007rt, with some indication of a weak narrow component in the earliest epochs (see second panel of Fig. 4). Unlike  $H_\alpha$ , the higher order Balmer lines,  $H_{\beta,\gamma}$ , do not appear to have a broad component. For  $H_\beta$  this is clearer, as it has a higher intensity relative to the strong blue continuum, but the behaviour of these lines are similar. The line profile of  $H_\beta$  has an emission peak with a FWHM of  $\sim 4000$  km s<sup>-1</sup> in the first epoch of data. This corresponds to the intermediate component seen in  $H_\alpha$ , and changes at a similar rate (see Fig. 7). In SN 1988Z, similar differences in the  $H_\alpha$  and  $H_\beta$  profiles were observed, with no broad component detected in the latter (Turatto et al. 1993). Blended with the  $H_\beta$  line is an absorption trough or depression in the continuum. Whilst there may be some contribution from hydrogen, the FWHM is twice the width of the emission in  $H_\beta$ , and it is unlikely to be due to hydrogen alone.



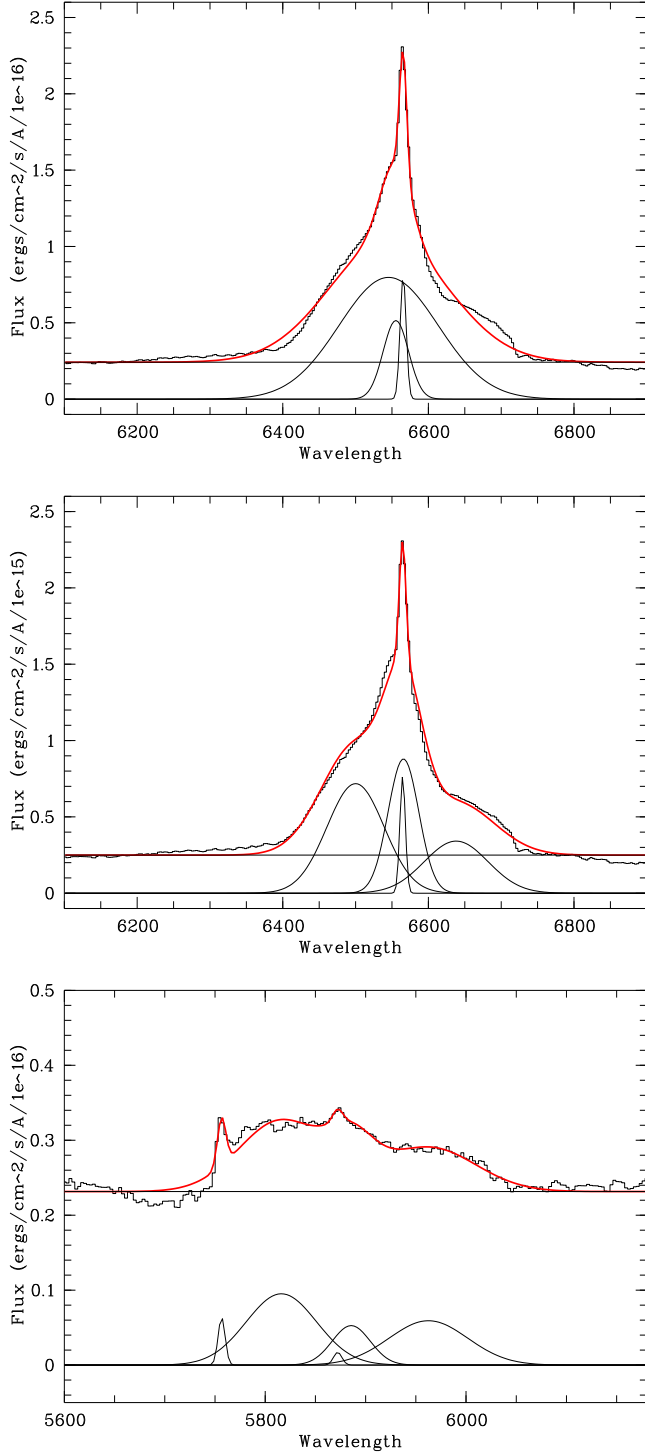


Fig. 6: Gaussian profile fits to  $H_{\alpha}$  and He I 5875 Å line from the day 131 spectrum of SN 2007rt. **Top Panel:**  $H_{\alpha}$  line is reproduced using a narrow, intermediate and broad component. Note the poor fit to the wings, in particular in the red part of the line. **Middle Panel:** Here 4 Gaussians are used to fit the  $H_{\alpha}$  line; a narrow and intermediate component and 2 higher velocity (broad) components shifted bluewards and red-wards relative to the intermediate and narrow features. **Lower Panel:** He I 5875 Å line from the day 131 spectrum fit with the same 4 Gaussians. Note that in addition to the multiple components of He I the left wing of the line is contaminated by narrow [N II] 5755 Å line.

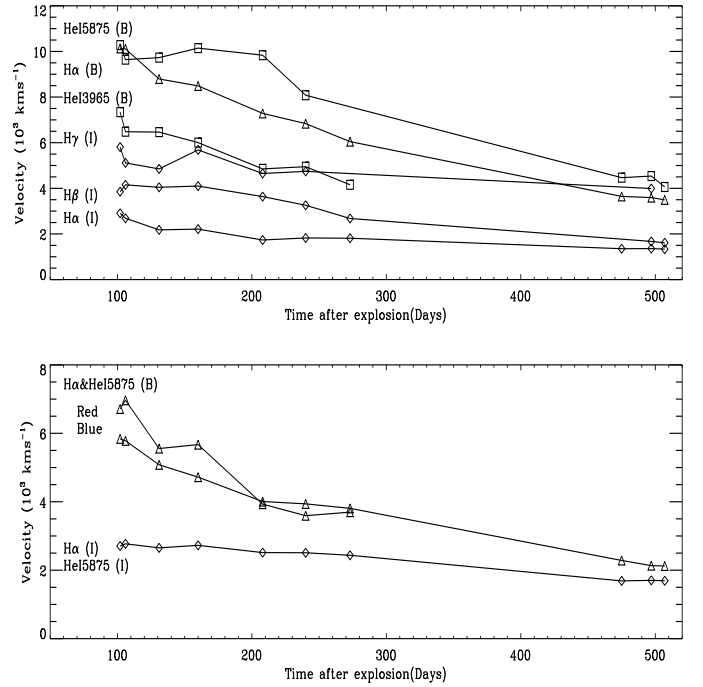


Fig. 7: Line velocities as a function of time after assumed explosion. **Upper panel:** velocities of He I 3965, 5875 Å, and  $H_{\gamma,\beta}$  using one Gaussian for the broad component as presented in Table 3. The broad and intermediate velocities of  $H_{\alpha}$  are plotted as determined using 3 Gaussians. The symbols represent:  $\square$  - broad He,  $\triangle$  - broad H,  $\diamond$  - intermediate H. **Lower panel:** velocities of the intermediate ( $\diamond$ ) and broad ( $\triangle$ ) blue and red shifted components of the 4 Gaussian fits to the  $H_{\alpha}$  and He I 5875 Å lines. The B & I in the parenthesis indicate the broad and intermediate component velocities, respectively. Note that in this latter fit the He and H components have the same velocities.

#### 4.4. Narrow emission lines

Besides the prototypical narrow  $H_{\alpha}$  feature, a number of other narrow emission features, many of which are forbidden lines, were observed in the low resolution spectra of SN 2007rt. These narrow lines have been identified as He I 5875, 7065 Å, [O III] 4363, 4959, 5007 Å, [N II] 5755 Å, [Ne III] 3866 Å, and very weak [Fe III] 5270 Å and [Fe VII] 6086 Å. There is also a possible detection of [Fe XI] 7891, although fringing in that part of the spectrum makes this identification marginal. Unfortunately the narrow lines were not resolved in our low resolution spectra. In the highest resolution spectrum in this low resolution group, taken on the 11<sup>th</sup> February 2008 the FWHM of the lines are typically a few 100 km s<sup>-1</sup> (see Table 5). The [O III] lines have velocities of  $\sim 200$  km s<sup>-1</sup>, which compares well with the narrow emission component of  $H_{\alpha}$ , suggesting they are produced in the same region of the CSM. An intermediate resolution spectrum of the  $H_{\alpha}$  region of SN 2007rt was obtained on the 4<sup>th</sup> February 2008 with ISIS/WHT and revealed additional narrow features of [O I] 6300, 6363 Å, [N II] 6548, 6583 Å and the high ionisation line [Fe X] 6374 Å. The [Fe VII] 6086 line was also clearly detected in this spectrum. In Table 5 the parameters of the gaussian fits to the narrow lines detected in the TNG spectrum on 11<sup>th</sup> February 2008 (day 160) and the ISIS/WHT spectrum (day 153) are presented as a guide to their parameters. Note that the

Table 5: Parameters of the Gaussian fits to the narrow lines detected in SN 2007rt from the day 153 and 160 spectra.

line	Day	$\lambda$ Å	FWHM km s <sup>-1</sup>	I 10 <sup>-15</sup> erg.s <sup>-1</sup> cm <sup>2</sup>
[Fe vii] 6086	153	6087.26	43	0.079
[O i] 6300	153	6300.63	47	0.090
[Fe x] 6374	153	6374.80	47	0.110
[N ii] 6548	153	6548.35	20	0.058
[N ii] 6583	153	6583.72	29	0.157
H $\alpha$ 6563 (e)	153	6562.43	84	8.84
Narrow (a)	153	6563.89	54	3.41
(e)	160	6561.80	213 (463)	3.97
[Ne iii] 3866	160	3865.03	289 (756)	0.596
[O iii] 4363	160	4358.23	198 (650)	0.317
[O iii] 4959	160	4956.10	(568)	0.187
[O iii] 5007	160	5008.36	(537)	0.480
N ii 5755	160	5754.09	(407)	0.47
He i 5875	160	5873.27	(396)	0.08
He i 7065	160	7066.50	185 (424)	0.252

The fwhm presented in parentheses are not corrected for resolution, all other values are.  
e- emission, a- absorption

velocities of the lines from the ISIS/WHT spectrum are significantly lower than derived from the lines in the spectrum taken seven days later, on the 11<sup>th</sup> February. This is due to the differences in the spectral resolution, as the lines in the low resolution spectra are unresolved. We note here that as the lines are unresolved there may be some unidentified contribution to these narrow emission lines from underlying H ii regions.

## 5. Discussion

In the introduction we mentioned the ambiguity surrounding the progenitors of Type IIn SNe and the debate over the mechanism for the SN 2002ic-like supernovae. The strong interaction in these so-called hybrid Type Ia/IIn objects makes it difficult to definitively conclude whether these are Type Ia or core-collapse supernovae. However in the case of SN 2007rt the presence of He in the ejecta, indicated by the broad He i 5875 Å line and the lack of broad forbidden Fe features at late phases, which are prominent in type Ia SNe, suggests that SN 2007rt is a core-collapse supernova.

### 5.1. Comparison with other interacting SNe

In Sect. 3 we noted the similarity between SN 2007rt and another type IIn supernova, SN 2005ip. At early stages this SN displayed a weak series of both low and high ionisation, narrow features (Smith et al. 2009a, see their Fig. 2), as detected here in SN 2007rt. SN 2005ip bears a strong resemblance to the prototype for the type IIn class, 1988Z, which also had a narrow, forbidden, emission line spectrum (Stathakis & Sadler 1991; Turatto et al. 1993). In SN 2005ip and 1988Z there is a strong narrow He i feature, with SN 2005ip developing an intermediate feature over time (Smith et al. 2009a, see their Fig. 8). SN 2007rt also has narrow He i 5875 and 7065 Å lines, which indicate the presence of helium in the circumstellar medium. However the main spectral difference between these two SNe is the presence of a broad He i 5875 Å feature in SN 2007rt.

This broad helium line is not usually detected in Type IIn spectra but is present in SN 2007rt from the first spectrum taken

~102 days post-explosion and narrows with time. A supernova with striking similarities to SN 2007rt is the type IIn SN 1997eg (Salamanca et al. 2002; Hoffman et al. 2008). In Fig. 8 these two supernovae are compared along with SN 2005ip and SN 1988Z. SN 1997eg has strong broad He i 5875 and 7065 Å lines with velocities comparable to the broad H $\alpha$  profile. Hoffman et al. suggest that the high He/H ratio in the ejecta of SN 1997eg, indicates that the progenitor star must have shed a significant amount of its hydrogen shell, possibly through an episode of mass-loss prior to the supernova explosion. This mass-loss episode would rid the star of a large quantity of its hydrogen shell and deposit the hydrogen rich material into its immediate environment, thus a helium rich atmosphere would be left behind in the progenitor star to be revealed in the supernova ejecta. We suggest that this is also a likely scenario for SN 2007rt. However, it should be noted that strong lines can be formed not just by a high abundance but are dependent on the temperature and density conditions of the material. Comparing the spectra of the four supernovae mentioned above, it is clear that there are varying degrees of He line strengths in these objects, with SN 2007rt being intermediate between SN 2005ip/SN 1988Z and SN 1997eg. One interpretation of this, is that there is varying degrees of H and He in the ejecta of these SNe. In addition to the high helium abundance, Hoffman et al. remarked that the peaked He profiles are suggestive of ejecta interacting with an asymmetric circumstellar medium, and this is substantiated by spectropolarimetry results.

At early times these type IIn supernovae have strong blue continua, with flatter red spectra. In the case of SN 2005ip a blackbody of 7300 K (Smith et al. 2009a) was required to fit the data. Our earliest spectrum of SN 2007rt, at 102 days post-explosion, was poorly fit by a blackbody with ~7550 K. Over time the blue excess decreased, and the red part of the spectrum flattened, making it difficult to fit a single blackbody. Smith et al. reported a similar effect in SN 2005ip. However, in this case the late time data resolved this continuum into a forest of high-ionisation (mainly Fe) emission lines. They suggest these lines are ionised by X-rays formed in the shocked material of a slow wind, and refer to a pseudo-continuum. This provides support for the suggestion that the blue excess in type IIn supernovae is related to the interaction of the ejecta with the CSM. Smith et al. suggest that the blue excess in SN 2006jc is a result of a similar effect, but the wind of the progenitor (likely a WR star) was faster, and hence the blue pseudo-continuum consisted of a blend of broader emission lines. If confirmed, this highlights the role the density and geometrical configuration of the progenitors wind plays in the evolution of these interacting SNe.

In the case of SN 2007rt the narrow H $\alpha$  line suggests that the progenitors wind has a velocity similar to that of SN 2005ip (~100 km s<sup>-1</sup>). The partially resolved features of O iii at 200 km s<sup>-1</sup> suggest we should be able to at least partially resolve a forest of narrow emission lines, if present. Nevertheless even at 507 days post-explosion we do not see this forest of narrow emission lines in the blue, despite the broad features in the continua of the two SNe being similar. The lack of evidence for this forest in our spectrum may be due to the continuum in SN 2007rt consisting of intermediate width emission lines, possibly of permitted/forbidden iron lines, formed in the shocked region. In Sect. 4.3 we noted the depression in the continuum to the blue of the H $\beta$  line. There is another such feature to the red of the [O iii 5007] Å line (see Fig. 9). These features are detected in many interacting supernovae such as 1997eg, 1995G, 2005la (Salamanca et al. 2002; Hoffman et al.

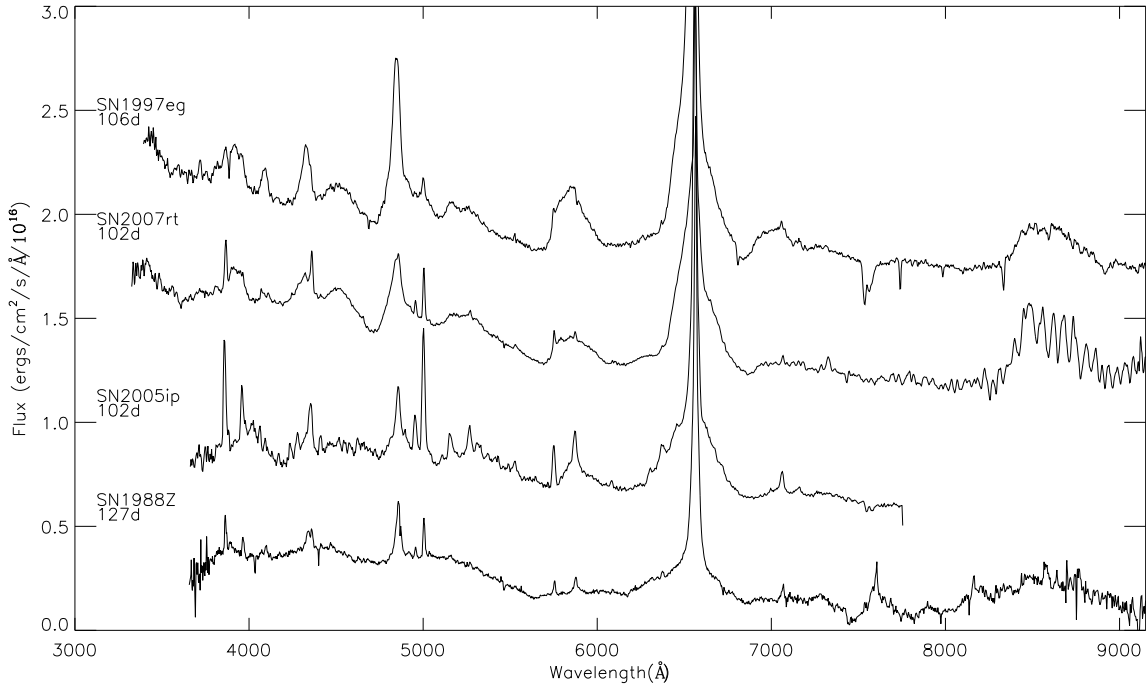


Fig. 8: Comparison of SN 2007rt, SN 2005ip, the type II<sub>n</sub> prototype, SN 1988Z, and an additional Type II<sub>n</sub>, SN 1997eg. Note the likeness of the underlying broad features of SN 2007rt, & SN 2005ip, suggesting that these two supernovae are of the same age at the given epoch. The data for SN 2005ip and SN 1997eg are unpublished spectra from the Padova-Asiago Supernova Archive, and that of SN 1988Z is from Turatto et al. (1993).

2008; Pastorello et al. 2002, 2008b, see their Fig. 4), and coincide well with the broad Fe II absorption features from multiplet 42 (4924, 5018, 5169 Å) present in type Ib/c spectra. However a comparison of late time spectra of SN 2007rt and SN 2005ip, as in Fig. 9, shows convincing evidence that in the spectra of interacting SNe this is due to a lack of emission lines amongst a dense forest, rather than an absorption trough. This is also thought to be the case for SN 2006jc (Pastorello et al. 2007). The non-blackbody like continuum, similarity in the broad features in the blue part of the spectrum with those of many interacting supernovae, and the clear case of a pseudo-continuum in SN 2005ip leads us to believe that SN 2007rt also has a pseudo-continuum. However we can not rule out that a real thermal continuum contributes wholly or partially to the early time spectra of SN 2007rt.

### 5.2. Properties of the CSM

The CSM electron density and temperature can be inferred from the narrow forbidden lines in the spectrum of SN 2007rt. Coronal lines, such as [FeX] 6374 Å, as well as low ionisation [O III] lines are present, suggesting that there are regions of the CSM with different temperatures and densities. This is not unexpected in the complex environment of the CSM, and the detection of high ionisation Fe lines indicates that X-rays are produced in the shocked region. The presence of [Fe VII] 6086 Å and [Fe X] 6374 Å combined with the absence of [Fe VI] suggests that these lines are formed in a region of the CSM with an electron temperature between  $2.5$  and  $8 \times 10^5$  K (Bryans, et al. 2008). The [O III] lines, however, are expected to form in cooler regions with electron temperatures of  $\sim 1 \times 10^5$  K (Bryans, et al. 2008). Using

the relationship between the [O III] lines and electron density by Osterbrock (1989), as cited in Salamanca et al. (2002), we can determine the density of the CSM. Thus using the temperature range implied above, with the [O III] line intensity ratio ( $I_{4959+5007}/I_{4363}$ ) of 2.93 the density of the CSM, where the [O III] lines form, is  $4.6 \times 10^7 \text{ cm}^{-3}$ .

The narrow  $H_\alpha$  component is present in the early spectra of SN 2007rt but has completely disappeared in the spectrum taken on 1<sup>st</sup> May 2008. If we assume that this is due to the ejecta having swept up the entire CSM, we can determine the extent of the CSM. Assuming the explosion date discussed in Sect. 3 and an ejecta velocity of  $10,000 \text{ km s}^{-1}$ , the unshocked region extends out to a maximum of  $2.13 \times 10^{16} \text{ cm}$ . Material ejected from a star at a wind speed of  $\sim 100 \text{ km s}^{-1}$  would take  $\sim 70$  years to reach such a distance, hence the mass-loss must have occurred on this timescale. However, given the high densities of the CSM, as implied above from the O III lines, it is possible that this narrow  $H_\alpha$  feature disappears due to recombination. This explanation has been given for the disappearance of such features in SN 1994aj and SN 1996L (Benetti et al. 1998, 1999).

### 5.3. Nature of the Progenitor Star

In Sect. 4.1 we discussed the very narrow P-Cygni feature detected in SN 2007rt, the absorption component of which has a FWHM of  $54 \text{ km s}^{-1}$ , and extends out to  $128 \text{ km s}^{-1}$ . Narrow P-Cygni profiles have been detected in a number of type II<sub>n</sub> SNe. However, they appear to fall into two different categories; those with very narrow profiles with the blue edge of the absorption profile extending out to  $< 200 \text{ km s}^{-1}$  and those with velocities in the range  $600\text{--}1000 \text{ km s}^{-1}$ . Some su-

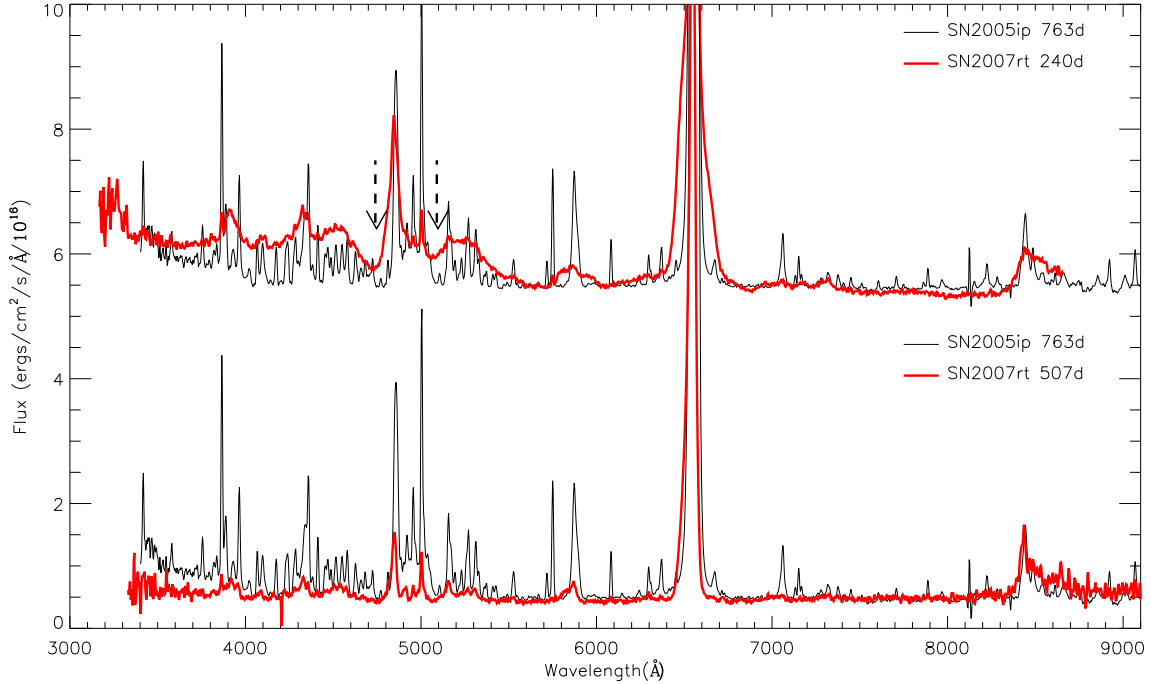


Fig. 9: Comparison of SN 2007rt at 240 days and 507 post-explosion (thick red line) with SN 2005ip at 763 days after explosion (thin black line). The data for SN 2005ip are unpublished spectra from the Padova-Asiago Supernova Archive.

pernovae which fall into the latter category are SNe 1994aj, 1994W, 1995G, and 1996L, while those with lower velocities are SNe 1997ab, 1997eg, 2005gj (Chugai & Danziger 1994; Sollerman et al. 1998; Benetti et al. 1998, 1999; Pastorello et al. 2002; Salamanca et al. 1998, 2002; Trundle et al. 2008). As mentioned in Sect. 4.1 these P-Cygni profiles provide insight into the stellar wind velocity of the progenitor star. The high velocities observed in SN 1994W and others are consistent with the wind velocities observed in WR stars (Crowther 2007). Luminous blue variables (LBVs) have slower wind velocities in the range of  $100\text{--}500\text{ km s}^{-1}$  (Stahl et al. 2001, 2003; Smith et al. 2007), which may explain some of the objects in the low velocity category, such as in the case of SN 1997ab. Typically red supergiants have velocities of approximately  $10\text{ km s}^{-1}$  but there are a few cases for which  $30\text{--}40\text{ km s}^{-1}$  edge velocities have been detected (viz. VY CMa see Smith et al. 2009b, and references therein). Therefore it cannot be ruled out that the wind velocities of some of these lower velocity objects may be consistent with extreme red supergiants. The expansion velocity of  $\sim 128\text{ km s}^{-1}$  is on the lower extreme of the LBV range, comparable to quiescent LBVs such as HD160529 (Stahl et al. 2003), and is quite high for red supergiants.

Type II spectra show no indication of He spectral lines at optical wavelengths, except for at very early stages ( $\sim 1$  week) when the high temperatures in the ejecta allow for their formation. Type IIb are the only SNe which have He and H present in their spectra, with possibly type Ib showing a trace of H accompanied by He. If the interpretation that the broad He I 5875 Å line in SN 2007rt is formed by a high helium abundance is valid, it suggests that the atmosphere of SN 2007rt’s progenitor has a higher He/H ratio than that of many Type II SNe progenitors. This places the progenitor of SN 2007rt as a transitional object between those of normal Type IIP’s and those of

hydrogen stripped core collapse SNe. The combination of H and He in the ejecta would suggest either the progenitor passed through an LBV phase and has lost a significant amount of its H shell through its previous mass-loss history or that the progenitor is in a more evolved WN or WNH phase, i.e. mass-loss via stellar winds has revealed H-burning products at the stars surface but not He-burning products as would be the case in WC stars. However, the very low (LBV-like) wind velocity of the unshocked material is not consistent with a WR wind, as velocities in such stars are typically greater than  $500\text{ km s}^{-1}$  (Crowther 2007, and references therein). If the progenitor is a WR star, the CSM detected by the narrow H components could be the result of an LBV outburst, which occurred prior to the progenitor entering a WN phase. In this case the progenitor would need to be in a very early stage of the WN phase, as otherwise the LBV wind would be swept up by the WN wind (van Marle et al. 2007). However we should note that there is no clear distinction between quiescent LBVs and WNH stars, as many of the latter are known to be quiescent LBVs (viz. AG Car, see Smith & Conti 2008c, and references therein).

#### 5.4. Explanation of the H and He I Asymmetries

As discussed in Sect 4.2, the H $\alpha$  and He I 5875 Å profiles in the spectra of SN 2007rt are peculiar. An asymmetry is present in these lines from the first spectrum onwards (see Fig. 4). In the last few epochs of our spectral dataset, from 240 days, a blueshift is detected.

##### 5.4.1. Late phase evolution: $\sim 240\text{--}507$ days post-explosion.

Once the temperature in the ejecta has dropped below the threshold for dust grains to condense, dust can form. The presence of

dust grains causes a net blueshift due to the absorption of redshifted light. Hence, asymmetric and blueshifted profiles formed as the ejecta expands and cools, can be explained by dust forming in the ejecta. In Fig. 4 it can be seen that the asymmetry of the  $H_\alpha$  profile in SN 2007rt increases with time and at late phases become blueshifted with significant absorption of the redshifted light. This behaviour appears to be consistent with the presence of newly formed dust. In addition there is an increasing asymmetry in the He I line. Evidence of such behavior due to dust has been seen in a number of Type II SNe, viz. 1987A (Danziger et al. 1989; Lucy et al. 1989). In SN 2007rt this blueshift is first detected in the spectrum taken on day 240 and becomes more pronounced by day 273. At even later epochs (475-507 days) the  $H_\alpha$  and He I 5875 Å lines show significant absorption of the redshifted light. Additionally, there is a significant decrease in SN 2007rt's magnitude during this late phase. The R-band magnitude declines at a rate of 0.01 mag  $d^{-1}$  from 458 to 562 days post-maximum. In the case of Type II SN 1987A a clear rise in the IR magnitudes was detected and is accompanied by a decline in the optical band at over 450 days post-explosion, indicating the formation of dust (0.016 mag  $d^{-1}$  at 467-562 days, Whitelock et al. 1989). Hence the formation of dust is the most probable justification for the decline in SN 2007rt's lightcurve in these latter points.

#### 5.4.2. Early phase evolution: ~102-240 days post-explosion.

The explanation of asymmetries in the H and He profiles in the earliest SN 2007rt spectra is uncertain, due in part to the uncertainty in its age. Here we outline two possible scenarios: (1) the object is young and can form dust in the fast expanding ejecta, (2) the broad components are inconsistent with the SNe's age and it has an asymmetric or bipolar outflow.

As mentioned above the reduced emission in the red wing of line profiles are suggestive of dust formation, however most dust detections have been made in late-time (~ 300 days) SNe spectra. The asymmetry in the first spectrum, taken approximately 102 days post-explosion, would appear to be inconsistent with the late-time formation of dust. Additionally if dust is invoked to explain the asymmetry in the profiles, an explanation for high ejecta velocities of 10,000 km  $s^{-1}$  at approximately 102 days after explosion is required due to the high energetic explosions implied by such velocities. Typically non-interacting core collapse supernovae have velocities of 10,000 km  $s^{-1}$  and greater only within 30 days of the explosion (Patat et al. 2001, see Fig. 5). At 100 days post-explosion, 7000-5000 km  $s^{-1}$  are more typical expansion velocities. Whilst the age of SN 2007rt is uncertain it is unlikely to be less than one month old, as the SN was first observed 21 days after discovery, was caught post-maximum, and in an interacting SNe such as this the spectrum is expected to be significantly bluer than detected (see Sect. 3.1).

Nevertheless assuming that SN 2007rt has an age significantly less than or equal to 100 days, it is difficult to form dust at an early epoch. Unlike the case of the peculiar Ibn SN 2006jc (Sakon et al. 2007; Mattila et al. 2008; Smith et al. 2008b; Di Carlo et al. 2008; Nozawa et al. 2008), the dust must have formed in the ejecta not in a post-shock region as the asymmetries observed are in the broad rather than the intermediate component. The only other object, for which dust has been invoked to explain early-time fading of the broad component, is SN 2005ip (Smith et al. 2009a). Smith et al. suggest that the dust forms in the fast expanding ejecta, however it is unclear what mechanism would allow for dust formation in the high temper-

ature gas of the ejecta. A possible added support to dust formation at a young age is the detection of IR excess by Fox et al. (2009) from NIR photometry of SN 2005ip from 50-200 days post-discovery.

An alternative scenario requires the presence of an aspherical or bipolar outflow. This scenario does not require such high expansion velocities as is the case above and hence is more consistent with our adopted explosion epoch. It also provides fits to the  $H_\alpha$  and He I 5875 Å lines, which are more consistent with their profiles. The profile fit in this case requires a blue and red-shifted component at velocities in the range 6000-7000 km  $s^{-1}$  with an additional intermediate and narrow component (see Fig. 6). The blue and red-shifted components represent high velocity material moving away from the SN, which may be indicative of a asymmetric outflow of material from the SNe. The profiles seen in SN 2007rt are reminiscent of the double-peaked profiles seen in Type Ib/c, viz. the broad-lined Ic, SN 2003jd, and the Type Iib, SN 2006T (Maeda et al. 2008; Valenti et al. 2008; Taubenberger et al. 2009). In the case of these latter objects the profile shapes can be explained by aspherical jet-like explosions viewed nearly sideways on (Mazzali et al. 2005; Maeda et al. 2008). Mazzali et al. and Maeda et al. suggest that these double-peaked features can be detected if viewed from angles of 60-90 degrees to the jet axis. For SN 2007rt, there is still a significant amount of H in the shell and any model would need to account for this.

## 6. Conclusions

We have presented a photometric and spectroscopic analysis of the Type IIn supernova SN 2007rt over more than 1 year after discovery. At 102 days post-explosion, SN 2007rt bears a striking resemblance to the type IIn supernovae SN 1988Z, SN 1997eg and SN 2005ip (Stathakis & Sadler 1991; Turatto et al. 1993; Aretxaga et al. 1999; Salamanca et al. 2002; Hoffman et al. 2008; Smith et al. 2009a), with strong narrow/intermediate/broad  $H_\alpha$  emission lines, a strong blue continuum, as well as weak narrow emission lines from neutral to highly ionised states (viz. He I, [O III], N II, [Fe VII], [Fe X]).

The narrow H lines indicate the presence of a H-rich CSM surrounding the SN. An intermediate resolution spectrum of the  $H_\alpha$  region resolved the narrow emission feature into a P-Cygni profile with an edge velocity of 128 km  $s^{-1}$ . This suggests the SN progenitor underwent mass-loss with velocities at the low end of those detected in LBV winds. The first spectrum contains a strong intermediate  $H_\alpha$  component suggesting the ejecta had already begun to interact with the CSM. This is supported by the light curve of SN 2007rt, as it evolves very slowly over the early epochs of our data, declining at a rate of 0.003 mag  $d^{-1}$ . By day 240 the narrow  $H_\alpha$  component has disappeared and provides an estimate of the maximum extension of  $2.13 \times 10^{16}$  cm for the unshocked CSM shell. Furthermore, a blue shift in the broad  $H_\alpha$  feature at this late stage suggests that dust has begun to form in the ejecta.

A broad He I 5875 Å component was also present in SN 2007rt. This is not a typical feature of SNe type IIn, and may be indicative of ejecta with a higher He/H ratio than generally observed in type IIn SNe. It is therefore possible that its progenitor is transitional between those of normal type II's and hydrogen stripped core-collapse SNe, which as a result of its previous mass-loss history has lost a large amount of its hydrogen shell. There is also a hint of He present in the CSM, and hence the progenitor may be a WNH star in an early stage of evolution

or an LBV which has lost a significant amount of H in previous mass-loss events. Throughout the spectral observations, the  $H_{\alpha}$  profiles show a strong asymmetry that increases over time, the red wing being dampened compared to the blue wing. The presence of dust in the ejecta beyond 240 days is clear, however what causes the asymmetry in the earlier spectra is less certain. Two possible scenarios are presented to account for this which cannot be distinguished by our current dataset: (1) the supernova is significantly younger than estimated and dust is formed through some unknown mechanism in the fast expanding ejecta or (2) an asymmetric or bipolar outflow viewed nearly side on accounts for the asymmetry in the early epochs. The first scenario is similar to that invoked for SN 2005ip by Smith et al. (2009a), however the mechanism for forming dust in the fast expanding ejecta is unclear. The second scenario relies on the SNe being older than one or two months and that the expansion velocity behaves like normal non-interacting core-collapse supernovae.

## 7. Acknowledgements

The authors are grateful for the feedback from the referee and to Daniel Mendicini and Martin Nicholson for providing a number of photometric data points ([http://ar.geocities.com/daniel\\_mendicini/index.html](http://ar.geocities.com/daniel_mendicini/index.html); <http://www.martin-nicholson.info/1/1a.htm>). In addition we are grateful for the support from Avet Harutyunyan at the TNG, La Palma. CT acknowledges financial support from the STFC. FPK is grateful to AWE Aldermaston for the award of a William Penney Fellowship. This paper is based on observations from a number of telescopes; 2.2-m Calar telescope at the German-Spanish Astronomical Center at Calar Alto operated jointly by the Max-Planck-Institut für Astronomie (MPIA) and the Instituto de Astrofísica de Andalucía (CSIC), 1.82m Copernico telescope at Asiago Observatory operated by Padova Observatory, ALFOSC owned by the Instituto de Astrofísica de Andalucía (IAA) and operated at the Nordic Optical Telescope under agreement between IAA and the NBI/AFG of the Astronomical Observatory of Copenhagen, WHT and the Italian Telescopio Nazionale Galileo (TNG) operated by the Isaac Newton Group, and the Fundacin Galileo Galilei of the INAF (Istituto Nazionale di Astrofisica) on the island of La Palma at the Spanish Observatorio del Roque de los Muchachos of the Instituto de Astrofísica de Canarias. Observations were also carried on with the 0.35-m SLOOH telescope at the Teide Observatory (Canary Islands, Spain). SLOOH (<http://www.slooh.com>) is a subscription-based website enabling affordable, user-friendly control of observatories in Teide, Chile, and Australia.

## References

Agnoletto, I., Benetti, S., Cappellaro, E., et al. 2009, *ApJ*, 697, 1348  
 Aldering, G., Antilogus, P., Bailey, S., et al. 2006, *ApJ*, 650, 510  
 Aretxaga, I., Benetti, S., Terlevich, R. J. et al. 1999, *MNRAS*, 309, 343  
 Benetti, S., Cappellaro, E., Danziger, I. J., et al. 1998, *MNRAS*, 294, 448  
 Benetti, S., Turatto, M., Cappellaro, E., et al. 1999, *MNRAS*, 305, 811  
 Benetti, S., Cappellaro, E., Turatto, M., et al. 2006, *ApJL*, 2, 129  
 Blondin, S. 2007, *CBET*, 1156  
 Bryans, P., Landi, E., Savin, D. W., et al. 2009, *ApJ*, 691, 1540  
 Cappellaro, E., Turatto, M., Tsvetkov, D. et al. 1997, *A&A*, 322, 431  
 Chevalier, R.A., & Fransson, C. 1994, *ApJ*, 420, 268  
 Chugai, N. N., & Danziger, I. J. 1994, *MNRAS*, 268, 173  
 Crowther, P. A. 2007, *ARA&A*, 45, 177  
 Danziger, I. J., Gouffes, C., Bouchet, P., & Lucy, L. B. 1989, *IAU Circ.*, 4796,  
 1  
 Di Carlo, E., Massi, F., Valentini, G., et al. 2002, *ApJ*, 573, 144  
 Di Carlo, E., Corsi, C., Arkharov, A. A. & et al. 2008, *ApJ*, 684, 471  
 Falco, E. E., Kurtz, M. J., Geller, M. J., et al. 1999, *PASP*, Vol. 111, 758, 438

Foley, R.J., Smith, N., Ganeshalingam, M., et al. 2007, *ApJ*, 657, L105  
 Fox, O., Skrutskie, M. F., Chevalier, R. A., et al. 2007, *ApJ*, 691, 650  
 Galama, T. J., Vreeswijk, P. M., van Paradijs, J., et al. 1998, *Nature*, 395, 670  
 Gal-Yam, A., et al. 2007, *ApJ*, 656, 372  
 Gal-Yam, A., & Leonard, D.C., 2008, *Nature*, 458, 865  
 Gerardy, C. L., Fesen, R. A., Nomoto, K., Garnavich, P. M. Jha, S., et al. 2002, *ApJ*, 575, 1007  
 Hamuy, M., Phillips, M. M., Suntzeff, N. B., et al. 2003, *Nature*, 424, 651  
 Hoffman, J. L., Leonard, D. C., Chornock, R., Filippenko, A. V., Barth, A. J., & Matheson, T. 2008, *ApJ*, 688, 1168  
 Kawabata, K. S., Tanaka, M., Maeda, K., 2009, *ApJ*, 697, 747  
 Kotak, R., Meikle, W. P. S., Adamson, A., & Leggett, S. K., 2004, *MNRAS*, 354, L13  
 Kotak, R. & Vink, J.S., 2006, *A&A*, 460, L5  
 Li, W. 2007, *CBET*, 1148  
 Lucy, L. B., Danziger, I. J., Gouffes, G., & Bouchet, P. 1989, in *Structure and Dynamics of the Interstellar Medium*, ed. G. Tenorio-Tagle, et al (Berlin: Springer-Verlag), 164  
 Maeda, K., et al. 2008, *Science*, 319, 1220  
 Matheson, T., Filippenko, A. V., Chornock, R., Ryan, C., Leonard, D. C., & Li, W. 2000, *AJ*, 119, 2303  
 Mattila, S., Meikle, W. P. S., & Lundqvist, P. 2008, *MNRAS*, 389, 141  
 Mazzali, P. A., et al. 2005, *Science*, 308, 1284  
 McKenzie, E. H., & Schaefer, B. E. 1999, *PASP*, 111, 964  
 Nozawa, T., Kozasa, T., Tominaga, N., et al. 2008, *ApJ*, 684, 1343  
 Ofek, E. O., Cameron, P. B., Kasliwal, M. M., et al. 2007, *ApJ*, 659, 13  
 Osterbrock, D.E. 1989, *Astrophysics of Gaseous Nebulae and Active Galactic Nuclei*, University Science Books, Mill Valley CA  
 Pastorello, A., Turatto, M., Benetti, S., et al. 2002, *MNRAS*, 333, 27  
 Pastorello, A., Smartt, S. J., Mattila, S., et al. 2007, *Nature*, 447, 829  
 Pastorello, A., Mattila, S., Zampieri, L., et al. 2008a, *MNRAS*, 389, 113  
 Pastorello, A., Quimby, R. M., Smartt, S. J., et al. 2008b, *MNRAS*, 389, 131  
 Pastorello, A., Kasliwal, M. M., Crockett, R. M., et al. 2008c, *MNRAS*, 389, 955  
 Patat, F., Cappellaro, E., Danziger, J., et al. 2001, *ApJ*, 900, 555  
 Prieto, J. L., Garnavich, P. M., Phillips, M. M., et al. 2007, *AJ*, submitted, (arXiv:0706.4088v1 [astro-ph])  
 Sakon, I., Wada, T., Ohya, Y., et al. 2007, *ApJ*, 692, 546  
 Salamanca, I., Cid-Fernandes, R., Tenorio-Tagle, G., et al. 1998, *MNRAS*, 300, L17  
 Salamanca, I., Terlevich, R., & Tenorio-Tagle, G. 2002, *MNRAS*, 330, 844  
 Schlegel, E. M. 1990, *MNRAS*, 244, 269  
 Schlegel, E. M., Finkbeiner, D. P., Davis, M. 1998, *ApJ*, 500, 525  
 Schmidt, B. P., Kirschner, R. P., Leibundgut, B., et al. 1994, *ApJ*, 434, 19  
 Smith, N., Li, W., Foley, R. J. et al. 2007, *ApJ*, 666, 1116  
 Smith, N., Chornock, R., Li, W., et al. 2008a, *ApJ*, 686, 467  
 Smith, N., Foley, R. J., & Filippenko, A. V. 2008b, *ApJ*, 680, 568  
 Smith, N., & Conti, P. S. 2008c, *ApJ*, 679, 1467  
 Smith, N., Silverman, J. M., Chornock, R., et al. 2009a, *ApJ*, 695, 1334  
 Smith, N., Hinkle, K. H., & Ryde, N., 2009b, *ApJ*, 137, 3558  
 Sollerman, J., Cumming, R. J., & Lundqvist, P. 1998, *ApJ*, 493, 933  
 Sollerman, J., Kozma, C., Fransson, C., et al. 2000, *ApJ*, 537, L127  
 Sparks, W. B., Macchetto, F., Panagia, N. et al. 1999, *ApJ*, 523, 585  
 Stahl, O., Jankovics, I., Kovács, J., & et al., 2001, *A&A*, 375, 54  
 Stahl, O., Gäng, T., Sterken, C. & et al., B. 2003, *A&A*, 400, 279  
 Stanishev, V. 2007, *Astron. Nachr.*, 328, No. 9, 948  
 Sthakakis, R. A., & Sadler, E. M. 1991, *MNRAS*, 250, 786  
 Taubenberger, S., & et al., *MNRAS*, 2009, accepted, (arXiv:0904.4632v2 [astro-ph])  
 Trundle, C., Kotak, R., Vink, J. S., & Meikle, W. P. S. 2008, *A&A*, 483, L47  
 Turatto, M., Cappellaro, E., Danziger, I. J., Benetti, S., Gouffes, C. & Delle Valle, M. 1993, *MNRAS*, 262, 128  
 Valentí, S., Benetti, S., Cappellaro, E., et al. 2008, *MNRAS*, 383, 1485  
 van Marle, A. J., Langer, N., & García-Segura, G. 2007, *A&A*, 469, 948  
 Whitelock, P. A., Catchpole, R. M., Menzies, J. W., et al. 1989, *MNRAS*, 240, 7

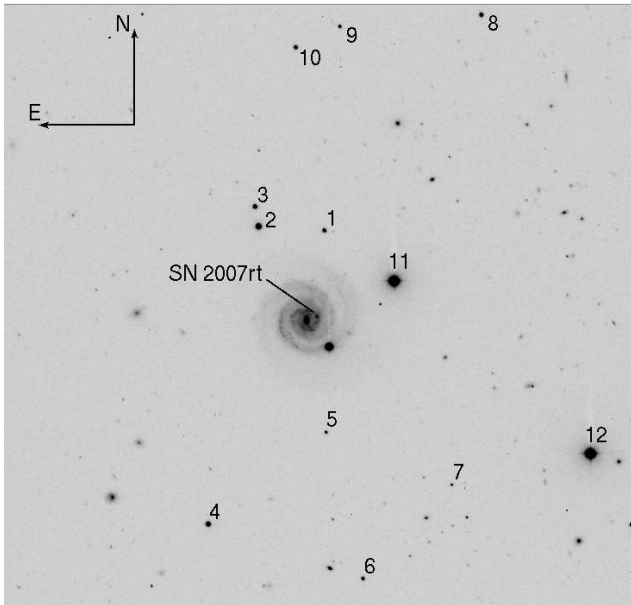


Fig. A.1: R band image of the region of SN 2007rt. Taken at CAFOS at Calar Alto on 19<sup>th</sup> March 2009.

#### Appendix A: Sequence Stars in local region of SN 2007rt

The sequence stars used to estimate the SN magnitudes are identified in Fig A.1 and their magnitudes are presented in Table A.1

Table A.1: UBVR magnitude of the sequence stars in the field of SN 2007rt.

ID	U	$U_{err}$	B	$B_{err}$	V	$V_{err}$	R	$R_{err}$	I	$I_{err}$
1	18.037	0.003	18.225	0.002	17.669	0.004	17.294	0.000	16.905	0.008
2	19.052	0.003	18.022	0.004	16.462	0.007	15.330	0.008	13.796	0.024
3	20.243	0.022	19.269	0.016	17.785	0.005	16.652	0.009	15.215	0.010
4	17.956	0.012	17.534	0.016	16.682	0.007	16.217	0.013	15.778	0.005
5	20.730	0.014	20.083	0.017	19.177	0.007	18.673	0.003	18.200	0.003
6	20.968	0.026	20.048	0.011	18.607	0.003	17.781	0.008	16.951	0.010
7	17.541	0.026	21.797	0.009	20.321	0.016	19.288	0.012	17.896	0.008
8	17.623	0.039	17.875	0.006	17.360	0.011	17.028	0.007	16.659	0.005
9	21.031	0.006	19.922	0.004	18.775	0.017	18.055	0.015	17.428	0.032
10	17.756	0.002	18.012	0.007	17.549	0.009	17.247	0.006	16.974	0.029
11			13.639	0.006	13.140	0.004				
12			13.792	0.007	13.064	0.009				



# Online Material

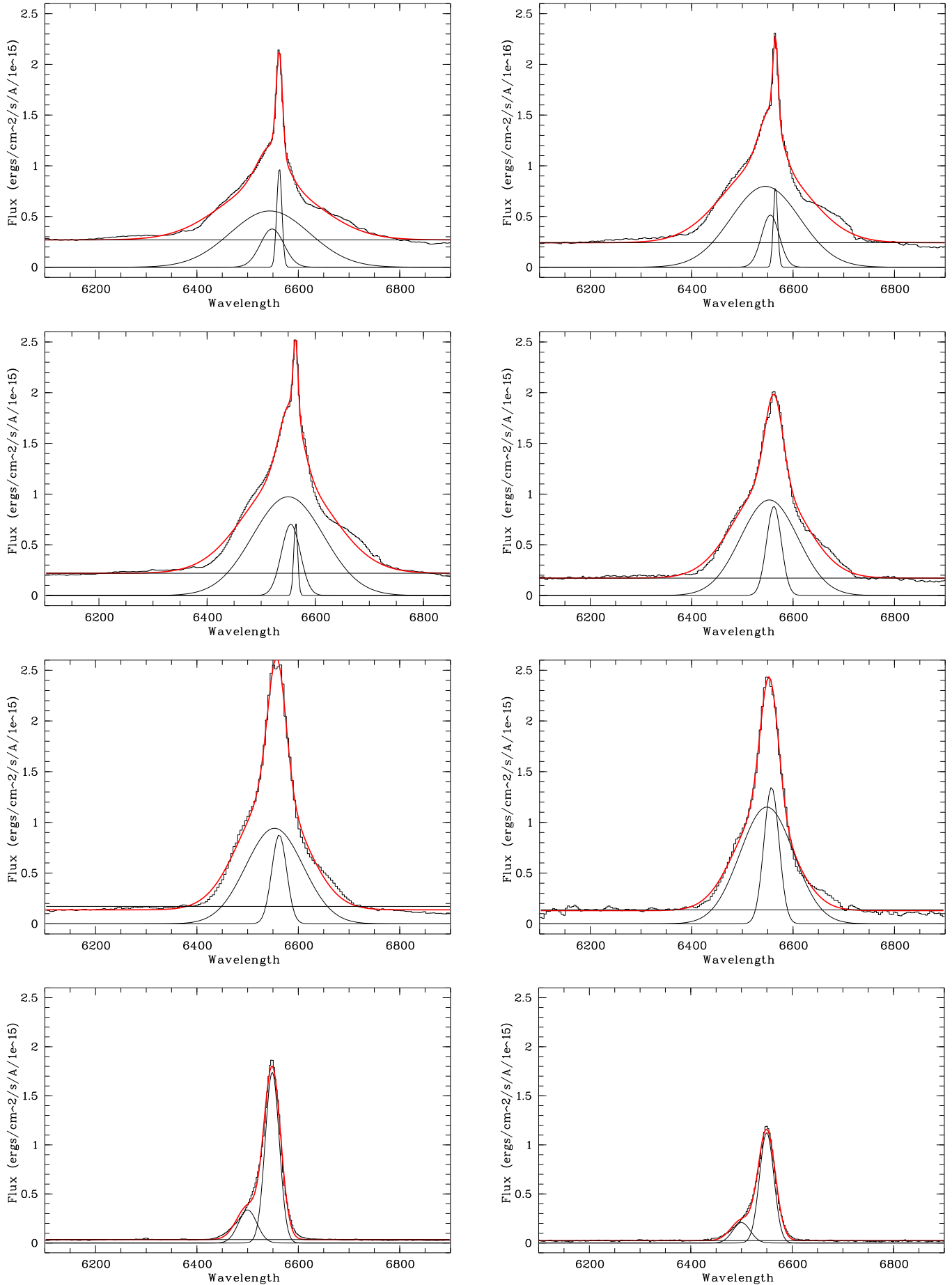


Fig. A.2: H $\alpha$  profile from each epoch (102, 131, 160, 208, 240, 273, 475, and 497 days after explosion going left-right from top to bottom). The profiles are decomposed into 2 or more components representing the broad, intermediate and narrow velocity components. Note that the data are plotted with a 1000 km/s velocity dispersion. The profiles are shown in the rest frame of the supernova.

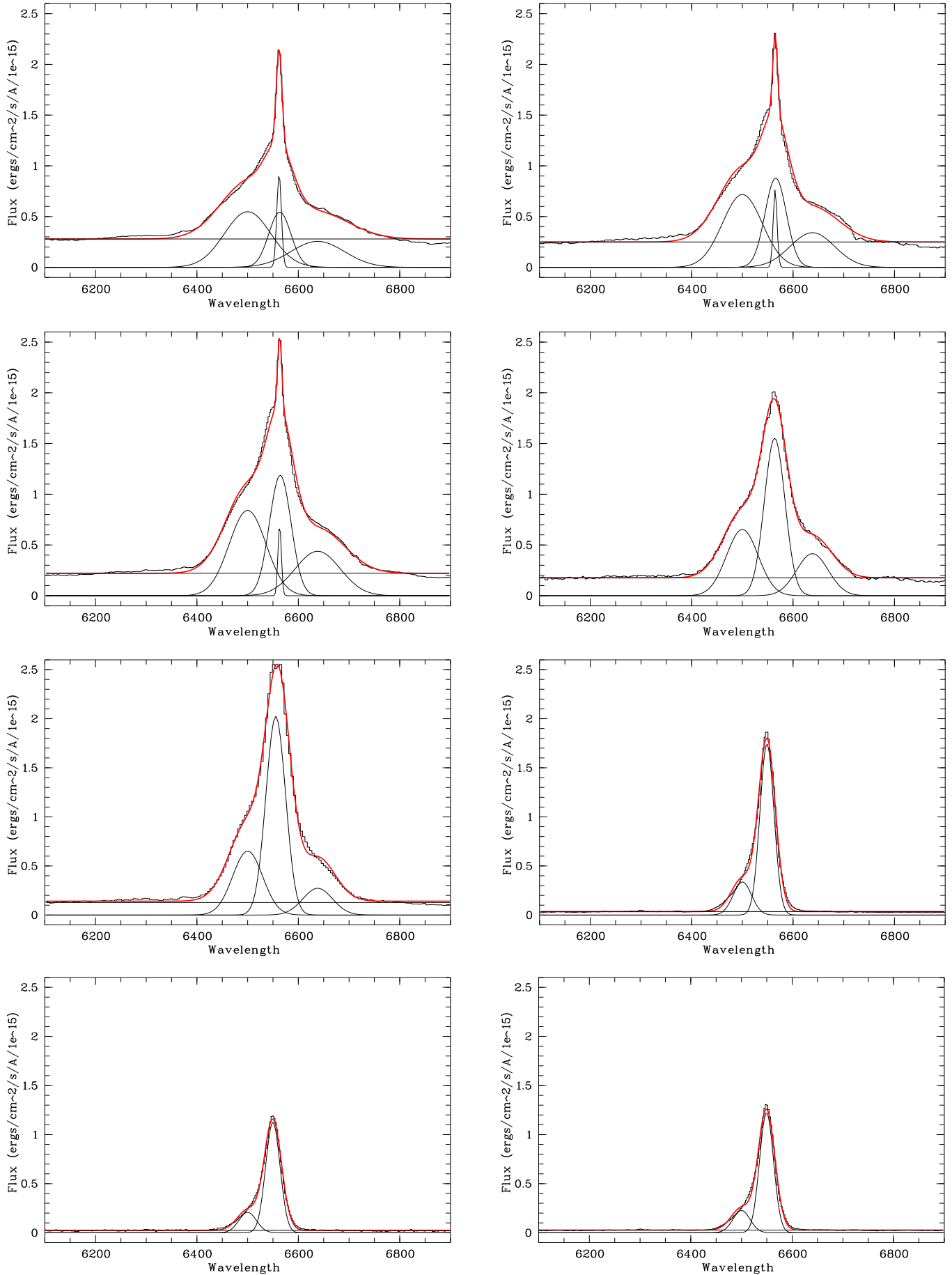


Fig. A.3: H $\alpha$  profile from each epoch (102, 131, 160, 208, 240, 475, 497, and 507 days after explosion going left-right from top to bottom) decomposed into 3 or more components representing the two broad, the intermediate and narrow velocity components. In the later spectra, only the broad and intermediate components are observed. Parameters for these fits are presented in Table 4.

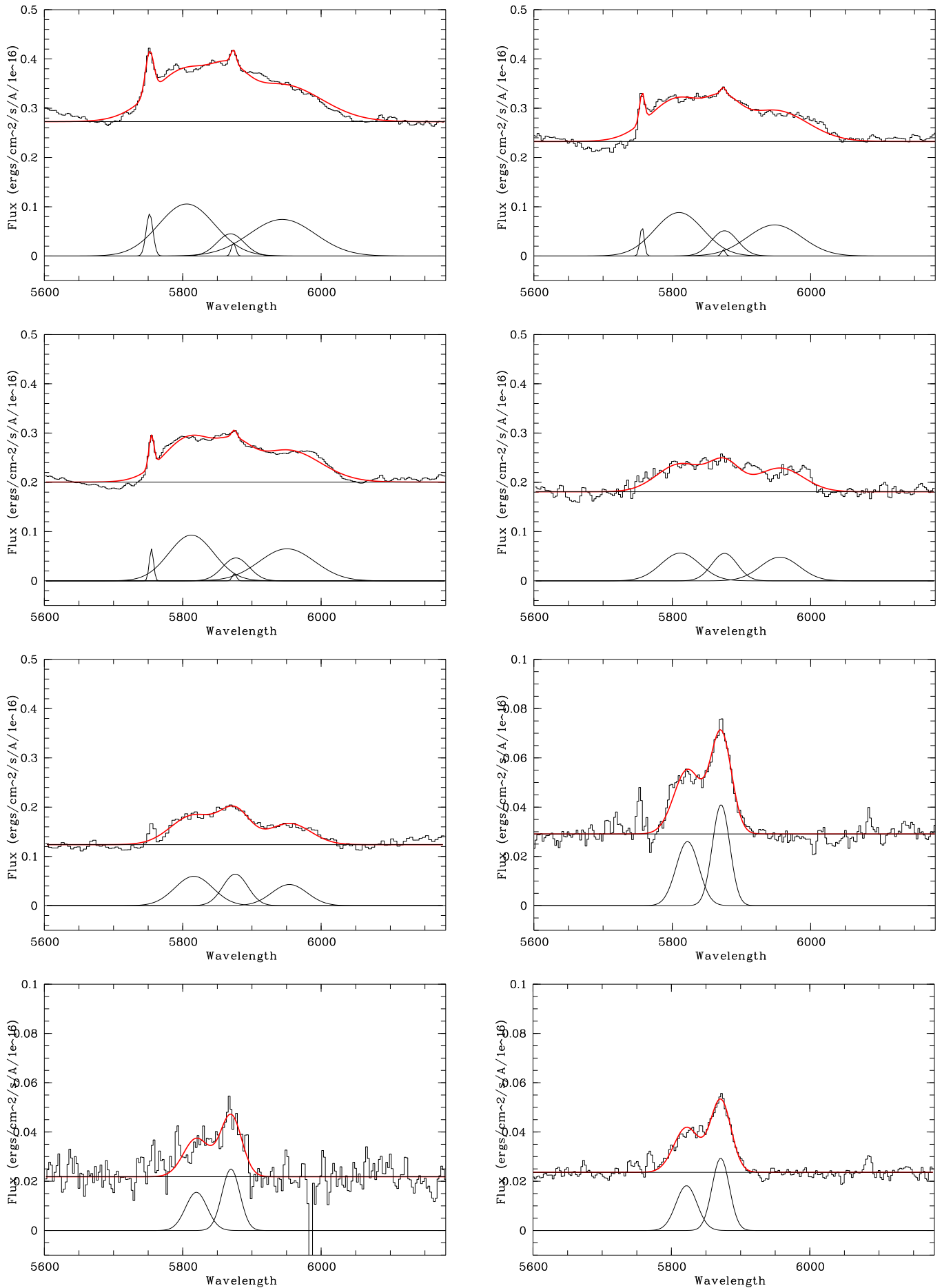


Fig. A.3: He I 5875 Å profile from each epoch (102, 131, 160, 208, 240, 475, 497, and 507 days after explosion going left-right from top to bottom) decomposed into 3 or more components representing the two broad, the intermediate and narrow velocity